

Tumorigenesis and Neoplastic Progression

# Simultaneous Expression of Caveolin-1 and E-Cadherin in Ovarian Carcinoma Cells Stabilizes Adherens Junctions through Inhibition of src-Related Kinases

Silvia Miotti,\* Antonella Tomassetti,\*  
Ileana Facetti,\* Elena Sanna,\* Valeria Berno,<sup>†</sup> and  
Silvana Canevari\*

From the Units of Molecular Therapies\* and Molecular Targets,<sup>†</sup>  
Department of Experimental Oncology and Laboratories, Istituto  
Nazionale per lo Studio e la Cura dei Tumori, Milan, Italy,  
Department of Molecular and Cellular Biology

**Cadherin-mediated adhesion plays an important role in maintaining cell-cell contacts and reducing tumor metastasis. However, neo-expression of E-cadherin in ovarian carcinoma does not prevent the release and spread of cells from the primary tumor. Because caveolin-1 is down-regulated concomitantly with E-cad expression, we investigated whether the stability of adherens junctions in ovarian carcinoma was affected by caveolin-1 expression. We used IGROV1 cells transfected with caveolin-1 (IGtC3), mock-transfected control cells (IGtM87), and SKOV3 cells that endogenously express caveolin-1. Simultaneous expression of caveolin-1 and E-cadherin favored membrane distribution of E-cadherin and its associated catenin (p120ctn), even when caveolin-1 was only focally associated with adherens junctions. Silencing of caveolin-1 induced intracellular E-cadherin redistribution in IGtC3 and SKOV3 cells. Treatment with the specific src kinase inhibitor PP1 increased E-cadherin expression in IGtM87 and SKOV3 cells and enhanced membrane localization of both E-cadherin and p120ctn. However, PP1 could not completely reverse the detrimental effects on cell-cell adhesion induced by Ca<sup>2+</sup> depletion in IGtM87 cells. Together, our data suggest that caveolin-1 expression indirectly promotes cell-cell adhesion in ovarian carcinoma cells by a mechanism involving inhibition of src-related kinases. Thus, down-regulation or loss of caveolin-1 might contribute significantly to the spread of tumor cells from the primary tumor. (*Am J Pathol* 2005, 167:1411-1427)**

Caveolin-1 (cav-1) is a 22- to 24-kd integral membrane protein present in numerous tissue types, which localizes in membrane subdomains called caveolae. Interaction of cav-1 with a variety of protein and nonprotein molecules results in pleiotropic effects on numerous cellular events such as signal transduction, gene regulation, lipid metabolism, and vesicular traffic.<sup>1-3</sup> Down-regulation of cav-1 in human tumor samples of different histological origin has been documented, suggesting that this protein has a negative regulatory role in tumor development and acts as an onco-suppressor.<sup>4-10</sup> Although cav-1-null mice are no more prone to tumor development than are the cav-1-expressing counterparts, the null mice reveal an increased susceptibility to dysplastic mammary<sup>11</sup> or epidermal lesions<sup>12</sup> in the presence of an initial oncogenic stimulus. However, in a few tumor histotypes, cav-1 up-regulation has been associated with tumor progression and enhanced metastatic capability.<sup>13,14</sup>

*In vitro*, cav-1 expression is up-regulated in confluent cells, and the protein distributes in areas of cell-cell contacts,<sup>15</sup> in which molecules involved in intercellular cell adhesion, such as E-cadherin (E-cad), are localized. E-cad mediates cell-cell adhesion through calcium-dependent homophilic interaction of the extracellular domains forming *cis*-dimers on the same cell, which interact with *cis*-dimers on neighboring cells to generate *trans*-interactions. Stable cell-cell interactions require binding of catenins (cat) to the cytoplasmic domain of E-cad. Commonly,  $\beta$ - or  $\gamma$ -cat bind the carboxy-terminal sequence of E-cad via armadillo-repeats and simultaneously interact with cytoplasmic  $\alpha$ -cat to link the entire complex to the

Supported by grants from Associazione Italiana Ricerca sul Cancro and the Cariplo Foundation.

Accepted for publication August 2, 2005.

Current address of V.B.: Department of Molecular and Cellular Biology, Baylor College of Medicine, Houston, Texas.

Address reprint requests to Silvia Miotti, Unit of Molecular Therapies, Department of Experimental Oncology, Istituto Nazionale Tumori, Via Venezian 1, 20133 Milan, Italy. E-mail: silvia.miotti@istitutotumori.mi.it.

cytoskeletal cortical actin ring.<sup>16,17</sup> Colocalization of cav-1 with E-cad/ $\beta$ -cat complexes at the cell junctions, co-fractionation in caveolae, and reciprocal co-immunoprecipitation of all of these molecules has been demonstrated in normal epithelial MDCKII cells.<sup>18</sup> E-cad is frequently down-regulated in epithelial tumors, with different mechanisms contributing at the transcriptional and post-transcriptional level to this down-regulation.<sup>16,17</sup> In cav-1-positive/E-cad-positive A431 carcinoma cells, continuous stimulation by epidermal growth factor (EGF) was shown to down-regulate the expression of both E-cad and cav-1 first at the membrane level through caveolae-mediated E-cad internalization and then at the transcriptional level with consequent activation of  $\beta$ -cat signaling.<sup>19</sup> In addition, NIH-3T3 cells co-transfected with cav-1 and  $\beta$ -cat showed inhibition of  $\beta$ -cat signaling.<sup>18</sup> Among the mechanisms involved in remodeling of the adherens junctions, tyrosine phosphorylation of adherens junction components mediated by both receptor and nonreceptor tyrosine kinases plays an important role.<sup>20</sup> In particular, tyrosine phosphorylation of  $\beta$ -cat and of p120ctn, the latter catenin binding to the E-cad cytoplasmic juxtamembrane region, reduces their respective affinity for the E-cad cytoplasmic domain<sup>21,22</sup> and enhances the disassembly of junctional complexes.

In the human normal ovary, the surface epithelium (OSE) is negative for E-cad expression<sup>23</sup> and displays a baso-lateral distribution of cav-1.<sup>5,10</sup> Cav-1 expression is frequently lost or down-regulated in malignant ovarian carcinomas,<sup>5,10</sup> whereas unlike in other carcinomas, E-cad is expressed *de novo* at least during early stages of tumor progression.<sup>23-25</sup> In the present study, we investigated the effect of the contemporaneous expression of cav-1 and E-cad on  $\beta$ -cat signaling, on subcellular distribution of cav-1 and cell-cell adhesion molecules, and on the stability of adherens junctions in ovarian carcinoma cells. Our overall results indicate that cav-1 does not contribute physically to the formation of adherens junctions, but promotes their stability by modulating the level and/or the subcellular distribution of E-cad and p120ctn through inhibition of src kinase activity.

## Materials and Methods

### Reagents and Antibodies

Phenylmethylsulfonyl fluoride, 3,3'-diaminobenzidine, Triton X-100 (TX-100), 2-(*N*-morpholino) ethanesulfonic acid (MES), Na<sub>3</sub>VO<sub>4</sub>, dimethylsulfoxide (DMSO), and aprotinin were from Sigma-Aldrich Fine Chemicals (St. Louis, MO); geneticin sulfate (G418) was from GIBCO-BRL (Paisley, Scotland); protease inhibitory cocktail and octyl- $\beta$ -glucoside (OG) were from Boehringer-Mannheim (Germany); the src inhibitor PP1 was from BIOMOL Research Laboratories (Plymouth Meeting, PA); and Tween 20 was from Merck (Hohenbrunn, Germany).

The following primary antibodies were used at the dilution recommended by the manufacturer: anti-cav 1 (rabbit), anti-lamin A/C Mab (mouse), anti-E-cad (rabbit), (Santa Cruz Biotechnology, Santa Cruz, CA); anti-E-cad

Mab (mouse), anti- $\beta$ -cat Mab (mouse) (Chemicon International, Temecula, CA); anti-tubulin- $\alpha$  Mab (mouse) (NeoMarkers, Inc., Fremont, CA); anti- $\beta$ -cat (rabbit), anti-actin (rabbit) (Sigma); anti-phosphotyrosine Mab (mouse) (Cell Signaling Technology, New England Biolabs, Beverly, MA), anti-p120ctn Mab (mouse), anti-p120ctn (pY228) phospho-specific Mab (mouse) (Transduction Laboratories, BD Biosciences Pharmingen, Palo Alto, CA); anti-E-cad clone HECD1 Mab (mouse) (Zymed Laboratories, Inc., San Francisco, CA); anti-src (pY418) (rabbit) (Biosource International, Camarillo, CA). Fluorochrome-conjugated Alexa Fluor 488 and Alexa Fluor 546 secondary antibodies were from Molecular Probes (Eugene, OR).

### Cell Cultures

The ovarian carcinoma cell lines IGtC3 and IGtM87, obtained by cav-1 cDNA or mock transfection, respectively, of E-cad-positive IGROV1 ovarian carcinoma cells<sup>5</sup> were used as a model to investigate how cav-1 expression affects E-cad/ $\beta$ -cat in ovarian carcinoma. IGtM87 and IGtC3 cells were maintained in folate-deficient RPMI 1640 medium (Sigma) supplemented with 10% fetal calf serum (FCS) (Sigma), 2 mmol/L l-glutamine (Sigma), and 400  $\mu$ g/ml G418. Ovarian carcinoma cell line SKOV3 was from ATCC (Manassas, VA). MDCKII cells were kindly provided by Dr. R. Sitia (Vita-Salute University-San Raffaele, DiBiT, San Raffaele Scientific Institute, Milan, Italy). Both SKOV3 and MDCKII cells were grown in standard RPMI 1640 medium (Sigma) supplemented with 10% fetal bovine serum and 2 mmol/L l-glutamine. Short-term cultured normal OSE cells were derived from scrapings at the time of the surgery for gynecological diseases other than ovarian carcinoma. Cells were cultured in 199-MCDB105 medium (Sigma) supplemented with 15% FCS, 2 mmol/L l-glutamine, and 25 mg/ml gentamicin as described.<sup>26,27</sup>

### Immunohistochemical Staining of Frozen Sections

All clinical specimens used in this study were obtained with Institutional Review Board approval and informed consent to use excess biological material for investigative purposes from all patients participating in the study. Tissue samples were obtained at the time of initial surgery, immediately frozen in liquid nitrogen, and stored at  $-80^{\circ}\text{C}$  until use. For immunohistochemical analysis, frozen 5- $\mu$ m serial sections were fixed in cold acetone: methanol (3:2) for 10 minutes and stained as described previously, with minor modifications.<sup>5</sup> Briefly, samples were preincubated for 20 minutes in phosphate-buffered saline containing 0.9 mmol/L CaCl<sub>2</sub> (PBS+), 1% bovine serum albumin (BSA), and 0.1% Tween 20, followed by incubation for 30 minutes at room temperature with primary antibody in PBS+ containing 1% BSA. PBS+/BSA alone was used as a negative control. Incubation with secondary biotinylated antibody in the same buffer was performed for 30 minutes at room temperature. Endogenous peroxidase activity was inhibited by incubation with

0.4% H<sub>2</sub>O<sub>2</sub> in PBS+ for 40 minutes. Bound antibodies were detected by using the avidin-biotin complex method (Vectastain kit; Vector Laboratories, Inc., Burlingame, CA) and 3,3'-diaminobenzidine as substrate.

### *Immunofluorescence Staining and Confocal Laser Microscopy*

Cells ( $3 \times 10^3$ /sample) seeded on glass coverslips were grown for 24 hours or 72 to 96 hours to obtain compact cell monolayers and fixed for 10 minutes in 10% cold methanol. After saturation in PBS+/BSA and 0.1% Tween 20, cells were incubated with primary antibodies, diluted in PBS+/BSA for 30 minutes at room temperature. After three washes in PBS+, secondary fluorochrome-conjugated (Alexa Fluor 488 and Alexa Fluor 546) antibodies in the same buffer were applied for an additional 30 minutes. Controls were exposed to relevant secondary antibodies alone and showed no significant degree of labeling. Coverslips were mounted on glass slides using MOWIOL-DABCO solution and analyzed by confocal microscopy (Microradiance 2000; Bio-Rad Laboratories, Inc., Hercules, CA) equipped with Ar (488 nm) and HeNe (543 nm) lasers. Images ( $1024 \times 1024$  pixels) were obtained using a 60 $\times$  oil immersion lens and analyzed using Lasersharp 2000 software. Reported images represent a single Z-section of the samples.

### *Subcellular Fractionation*

Confluent cells were washed in PBS+ containing 0.1 mmol/L Na<sub>3</sub>VO<sub>4</sub>, detached by scraping in hypotonic buffer HB-7 (5 mmol/L Tris, 1 mmol/L EDTA, 1 mmol/L dithiothreitol, and 11% sucrose, pH 7.4), and passed through a 0.3-mm-gauge needle. The cell lysate was centrifuged for 10 minutes at 3000 rpm in a SS34 rotor (Sorvall) at 4°C. The pellet was resuspended twice in the same buffer and pelleted under the same conditions. The last pellet was considered the nuclear fraction (Nu). Supernatants derived from nuclear pellet washings were pooled and centrifuged at 14,000 rpm in the same rotor as above for 45 minutes at 4°C. The pellet, washed once in the same buffer, represents the crude membrane fraction (M), whereas the pooled supernatants constitute the cytosolic fraction (Cy). The Nu and M pellets were each resuspended in the same buffer volume. Protein concentration was determined by BCA protein assay (Pierce, Rockford, IL), according to the manufacturer's protocol. Possible contamination of each fraction with proteins of other subcellular compartments was monitored using Western blot analysis for the presence of  $\alpha$ -tubulin and lamin A/C as markers of cytosol and nuclei, respectively.

### *Cells Transfection and Luciferase Assay*

Cells ( $1.2 \times 10^5$ ) were seeded in 12-well plates and transfected the following day using positively charged liposomes (kindly provided by Silvia Arpicco [University of Turin, Italy]) in the absence of FCS. TOP- or FOP-

FLASH constructs (2.5  $\mu$ g) (Upstate Biotechnology, Lake Placid, NY) containing three copies of the wild-type or mutated T cell factor (TCF) DNA-binding site, respectively, were co-transfected with the pRL-SV40 vector (0.01  $\mu$ g; Promega, Madison, WI) as a control for transfection efficiency. Firefly and Renilla Luciferase activities were evaluated on cell lysates using the DUAL-luciferase Reporter Assay (Promega), essentially as suggested by the manufacturer.

### *Separation of Lipid Rafts by Sucrose Gradient*

Cells were grown to confluence in T75 flasks to enhance localization of cav-1 at the cell-cell contacts. After three washes in cold PBS+, cells were lysed in 1% TX-100 containing buffer (25 mmol/L MES, pH 6.5, and 150 mmol/L NaCl), and the lysate was mixed 1:1 with 80% sucrose solution. Gradient fractionation (5–30%) and protein separation were carried out as described previously.<sup>28,29</sup> After ultracentrifugation for 17 hours in SW41 Beckman rotor, twelve 1-ml fractions were collected from the top of the gradient, and the distribution of relevant proteins was analyzed by SDS-PAGE<sup>30</sup> and Western blotting. The glycosyl phosphatidyl inositol (GPI)-anchored folate receptor<sup>29</sup> was used as a marker of lipid rafts.

### *Separation of Triton-Insoluble E-cad/ $\beta$ -cat Complexes*

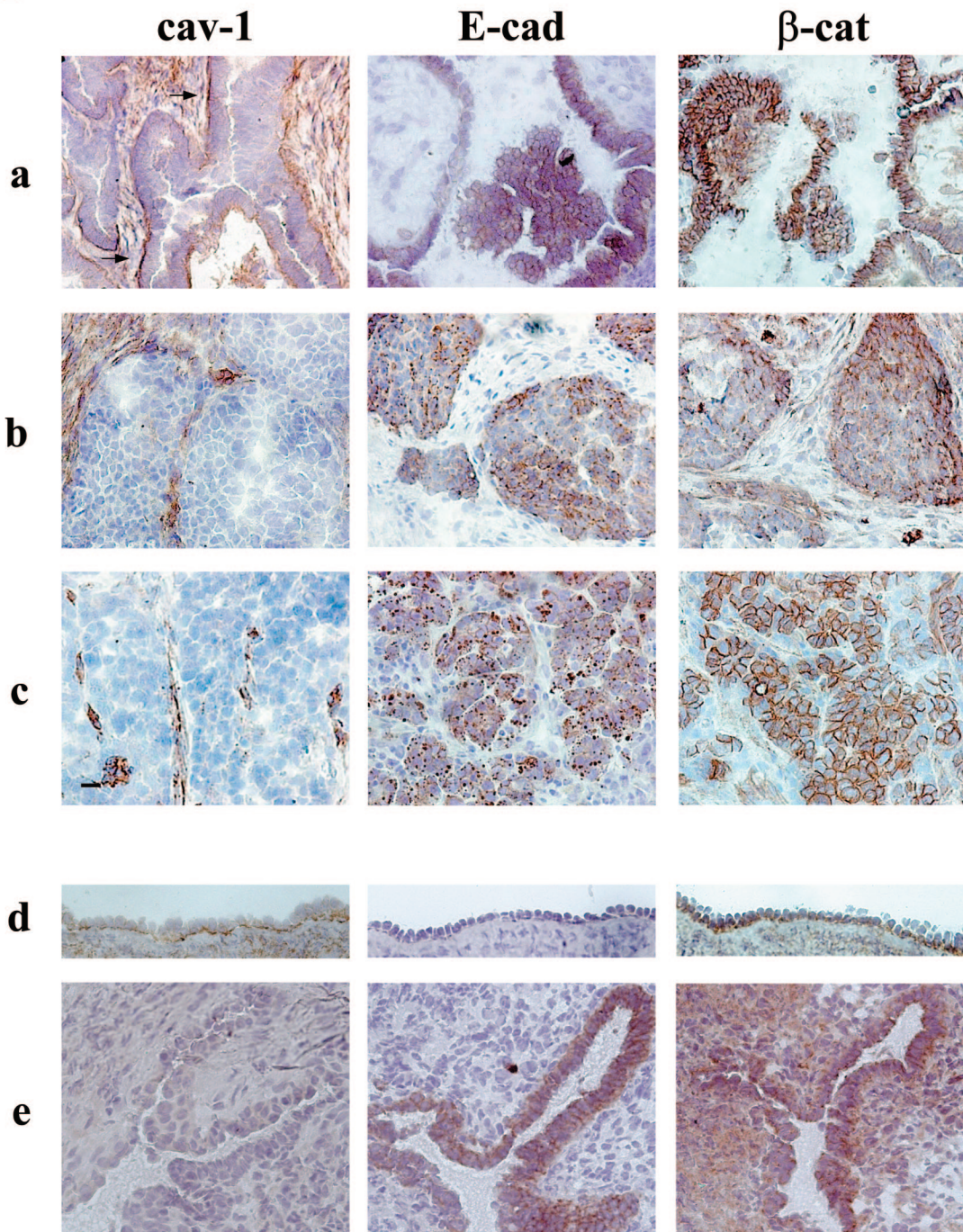
Confluent cells in T75 flasks were rinsed twice with cold PBS+ containing 0.1 mmol/L Na<sub>3</sub>VO<sub>4</sub> and treated in flasks for 10 minutes at 4°C with lysis buffer (25 mmol/L MES, pH 6.5, 150 mmol/L NaCl, 3 mmol/L MgCl<sub>2</sub>, protease inhibitor cocktail) containing 0.5% TX-100 and 1 mmol/L Na<sub>3</sub>VO<sub>4</sub>. After recovery of TX-100 solubilized proteins (TX-sol), cells in flasks were further treated for 30 minutes at 4°C with the same volume of the above buffer containing 1.1% OG (OG-sol). Both treatments were applied with gentle agitation. The solubilized fractions (TX-sol and OG-sol) were clarified by centrifugation (15,000  $\times g$  for 15 minutes) at 4°C, and the supernatant was recovered.

### *Immunoprecipitation, SDS-PAGE, and Western Blot Analysis*

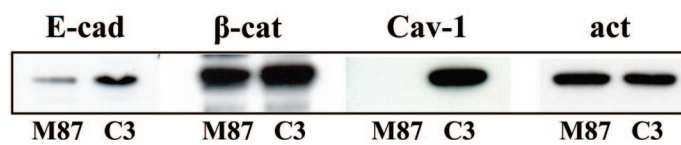
Immunoprecipitation of the bottom fractions (pool 9–12) of the sucrose gradient and from TX-sol, OG-sol fractions was carried out using magnetic beads conjugated with goat anti-mouse and sheep anti-rabbit antibodies (Dyna-beads; Dynal ASA, Oslo, Norway) as described.<sup>29</sup> Briefly, 1 to 2  $\mu$ g of each antibody was used for 25  $\mu$ l of beads. Normal mouse and rabbit sera were used as negative controls. Beads were incubated with the cell lysate for 3 hours or overnight at 4°C with rotation. After incubation, the beads were washed once with cold lysis buffer, twice with PBS+/BSA and protease inhibitors, and once with PBS+ plus inhibitor (10 minutes/wash). Bound material, eluted from beads by boiling for 5 minutes at 95°C in final



**A**



**B**



sample buffer containing 0.5% SDS, was analyzed by SDS-PAGE to 10% slab gels or in 4 to 12% precasted mini gels (Invitrogen, Paisley, UK).

Separated proteins were transferred on nitrocellulose sheets (Amersham Bioscience-GE Healthcare, Italy) for 2 hours at constant 200 mA. Staining with red ponceau (Sigma) was used to confirm homogeneous protein loading and transfer. After blocking in Blotto (5% nonfat dry milk; Merck), sheets were immunoreacted with the relevant primary antibodies and peroxidase-conjugated secondary antibodies (Amersham Bioscience-GE Healthcare) as described previously.<sup>29</sup> Reactivity was usually revealed by the ECL method (Amersham Bioscience-GE Healthcare). ECL plus was used to detect the phosphorylated forms of p120ctn. The Benchmark prestained protein ladder, used as a molecular mass standard, was from Invitrogen.

## Cell Treatments

### Inhibition of *src* Activity

Cells were grown for 2 to 3 days to 50 to 60% confluence, and for another 2 days in the presence of the *src* family inhibitor PP1. PP1 stock solution, dissolved in 100% DMSO, was diluted at least 1000-fold into culture medium to final concentrations of 20, 4, and 0.8  $\mu\text{mol/L}$ . Control cells were treated with culture medium containing DMSO at the same dilution. For immunofluorescence analysis, cells grown for 2 days on glass coverslips were treated with 4  $\mu\text{mol/L}$  PP1 and stained with relevant antibodies as described above. For analysis of protein expression, cells grown in flasks were sequentially solubilized as described above. Solubilized proteins were analyzed by SDS-PAGE and Western blotting as single extracts (TX-sol or OG-sol) or as a pool obtained by mixing the same volume of each.

### Adhesion Assay

IGM87 and IGtC3 cells were seeded in 24-well plates ( $5 \times 10^4$  cells/well) in RPMI 1640 medium, incubated at 37°C for 1 or 2 hours. After three vigorous PBS washings, adherent cells were fixed in cold methanol for 10 minutes, stained with 0.5% crystal violet in 20% methanol, and assessed for eluted stain at 550 nm. Background staining of wells without cells was subtracted from specific readings.

### $\text{Ca}^{2+}$ Depletion

Cells were grown, as described, for 2 days on glass coverslips and treated with 4  $\mu\text{mol/L}$  PP1 or DMSO-containing control medium and allowed to grow for another 2 days. After removal of culture medium, cells were incubated for 90 minutes at 37°C in the presence of PBS containing high (1 mmol/L) or low (0.030 mmol/L)  $\text{Ca}^{2+}$  concentrations, fixed in cold methanol, and immunostained for E-cad expression.

### Silencing of *cav-1* Expression by Short-interfering RNA (siRNA) Transfection

Cells ( $5 \times 10^4$ /sample) seeded on glass coverslips were grown for 24 hours at 37°C, washed in medium without FCS, and then transfected with 20 or 40 pmol (IGtC3 and SKOV3, respectively) of siRNA oligonucleotides specific for *cav-1* or with unrelated scramble (SCRB) sequence oligonucleotides (Dharmacon, Lafayette, CO) using lipofectamine 2000 (Invitrogen) (1  $\mu\text{l}$ /20 pmol oligonucleotides). After 7 hours, transfection reagents were removed and replaced with RPMI 1640 medium containing 10% FCS. Sixty-four hours later, cells were processed for immunofluorescence staining or solubilized for Western blot evaluation of *cav-1* silencing.

## Results

### The Pattern of *cav-1* and E-cad Expression in Ovarian Carcinoma Originates in Premalignant Early Modifications of Ovarian Surface Epithelium

Frozen sections from a panel of 11 human ovarian carcinoma, including 9 serous and 2 endometrial histotypes, were tested by immunoperoxidase staining with antibodies directed against *cav-1*, E-cad, and  $\beta$ -cat (Figure 1A). Cav-1 staining of tumor cells was absent in four cases and in five cases was only faint and focal. In the remaining two cases, marked basal reactivity of anti-*cav-1* antibody on tumor cells was observed. This pattern of reactivity was associated with the distribution of both E-cad and  $\beta$ -cat at the membrane level in correspondence with cell-cell contacts (sample a is representative of this pattern). All samples were E-cad positive, but a heterogeneous cellular distribution of the protein was observed; E-cad was present in both the membrane and intracellu-

**Figure 1.** Cav-1 expression modulates the expression patterns of E-cad in ovarian normal and malignant cells. Acetone-methanol-fixed sections were immunoreacted with anti-*cav-1* (rabbit), anti-E-cad (mouse), and anti- $\beta$ -cat (mouse) primary antibodies. Reactivity was revealed by immunoperoxidase staining. No reactivity was detected in control sections stained with anti-rabbit and anti-mouse secondary antibodies alone (not shown). **A:** Serous ovarian carcinoma (**a**, **b**, and **c**) representative of three different patterns of expression of the relevant molecules; normal ovary surface epithelium and an inclusion cyst of the ovary (**d** and **e**, respectively) stained for the relevant molecules. Tumor with basal-localized *cav-1* (**a**) (see **arrows**) shows E-cad and  $\beta$ -cat at the cell-cell contacts, whereas tumors that do not express *cav-1* have intracellular and membrane/intracellular distribution of E-cad and  $\beta$ -cat, respectively (**b** and **c**). Basally polarized *cav-1* is present in normal OSE (**d**), which appears E-cad-negative. By contrast, the neo-expression of E-cad in an inclusion cyst of the ovary (**e**) is associated with the loss of *cav-1* staining. Original magnification,  $\times 20$  in **a**, **b**, and **c**;  $\times 40$  in **d** and **e**. **B:** Immunoblot of lysates derived from confluent IGM87 and IGtC3 cells compared for expression of the indicated proteins. Note the slightly higher expression of E-cad in *cav-1*-positive IGtC3 than in control IGM87 cells. A representative experiment of four is reported.



larly (five cases), or in the membrane only (two cases), or intracellular only (four cases). All samples but one revealed  $\beta$ -cat expression, and in most of the tumors (9 of 11),  $\beta$ -cat was detected in both the membrane and in the cytoplasm. In the absence of cav-1, two different patterns of E-cad and  $\beta$ -cat expression were observed; both E-cad and  $\beta$ -cat were present intracellularly (sample b) or  $\beta$ -cat was present at the cell membrane and E-cad was intracellular (sample c). In addition to confirm cav-1 down-regulation in ovarian tumors, these results indicate that E-cad is not necessarily associated with the cell membrane and that  $\beta$ -cat can localize at a site independent of that of E-cad. Moreover, the findings suggest that when cav-1 is present and basally polarized, both E-cad and  $\beta$ -cat localize at the membrane.

Similar analysis of OSE revealed the polarized baso-lateral expression of cav-1 (Figure 1A, sample d). Clefts and inclusion cysts of the ovary, which are thought to originate epithelial ovarian tumors, revealed not detectable cav-1 in the invaginated epithelium (8 of 8 inclusion cysts and clefts examined) (sample e). Only the invaginated epithelium displayed neo-expression of E-cad (sample e), whereas both normal and cystic epithelium (sample d and e, respectively) expressed  $\beta$ -cat in a baso-lateral distribution.

To investigate how cav-1 expression might affect the E-cad/ $\beta$ -cat system in ovarian carcinoma cells, we used as a model the ovarian carcinoma cell line IGROV1 transfected with cav-1 cDNA (IGtC3) and the corresponding mock-transfected, cav-1-negative (IGtM87) cells.<sup>5</sup> Both cell lines were positive for E-cadherin expression. In standard growth conditions, those cell lines have similar levels of E-cad mRNA, as evaluated by real time PCR (data not shown), whereas IGtC3 cells by Western blot expressed slightly more E-cad protein than IGtM87 cells (fold increase, 1.5; range, 1 to 3.1), as evaluated in four independent experiments (Figure 1B).

### *Cav-1 Expression in IGROV1 Ovary Carcinoma Cells Modulates neither the Subcellular Distribution nor Signaling Activity of $\beta$ -cat*

In contrast with previous data,<sup>18</sup> cav-1 expression in our experimental model did not appear to affect  $\beta$ -cat nuclear distribution or transcriptional activation. Subcellular fractionation analysis revealed  $\beta$ -cat in the nuclear, membrane, and cytoplasmic fractions of both cell lines. The ratio between nuclear and membrane-associated protein remained unchanged after cav-1 transfection (Figure 2A). More importantly, analysis of the transcriptional activity of the  $\beta$ -cat/TCF complex, using the TOP- and FOP-Flash reporter genes, showed no transcriptional activity (Figure 2B) of the reporter gene constructs even in mock-transfected IGtM87 cells, indicating that the  $\beta$ -cat/TCF complex is not functional in these cells although slight TCF4 expression was detected (data not shown).

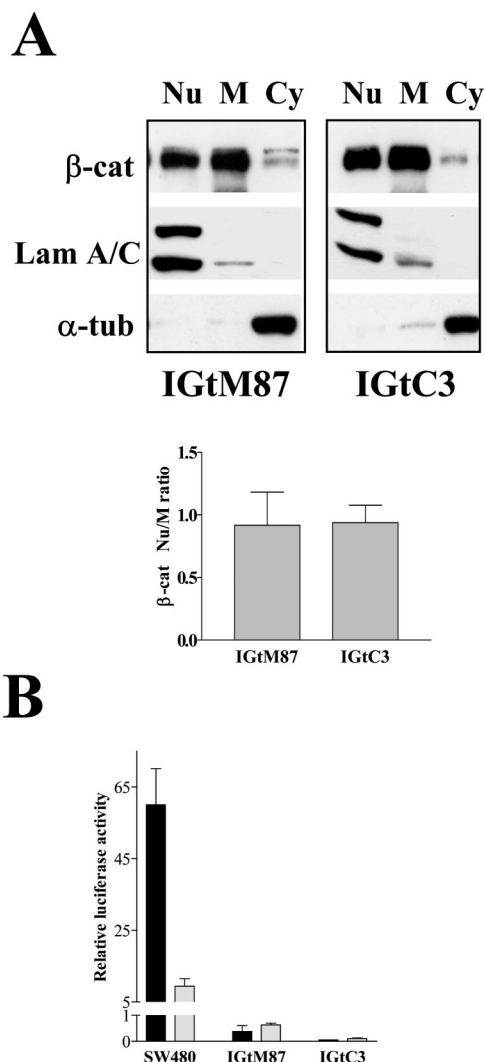


**Figure 2.** Cav-1 expression in ovary carcinoma cells does not affect  $\beta$ -cat expression and signaling. Nuclear (Nu), membrane (M), and cytosolic (Cy) fractions were obtained from confluent IGtM87 and IGtC3 cells by hypotonic cell lysis and differential centrifugations (see Materials and Methods). Each fraction (10  $\mu$ g) was analyzed by SDS-PAGE and Western blot. The nuclear marker lamin A/C and the cytosolic marker  $\alpha$ -tubulin were used to check the fractionation. **A:** A representative experiment that reveals no change in the  $\beta$ -cat Nu-to-M ratio in IGtC3 cells as a consequence of cav-1 transfection. The Nu-to-M ratio (mean  $\pm$  SD) was calculated by densitometric evaluation in four independent experiments. **B:** To evaluate  $\beta$ -cat/TCF transcriptional activity, IGtM87 and IGtC3 cells were transiently transfected with TOP- and FOP-FLASH constructs (containing wild-type or mutated TCF DNA-binding site, respectively), and promoter activities were determined. SW480 cells were tested in parallel as a positive control for  $\beta$ -cat/TCF transcriptional activity.  $\blacksquare$ , TOP-FLASH;  $\square$ , FOP-FLASH. Error bars represent the mean  $\pm$  SD from triplicate plates.

### *Cav-1 Localizes at Cell-Cell Contacts and Co-Precipitates with E-cad/ $\beta$ -cat Complexes but Is Not Associated with Lipid Rafts*

To examine possible interactions of cav-1 at the membrane level with E-cad/ $\beta$ -cat complexes, we monitored the distribution of E-cad,  $\beta$ -cat, and, when present, cav-1 in IGtM87 and IGtC3 cells at different times of growth by epi-fluorescence analysis (Figure 3). Irrespective of cav-1 expression, E-cad did not appear to be present at the cell junctions but did appear to be still located intra-

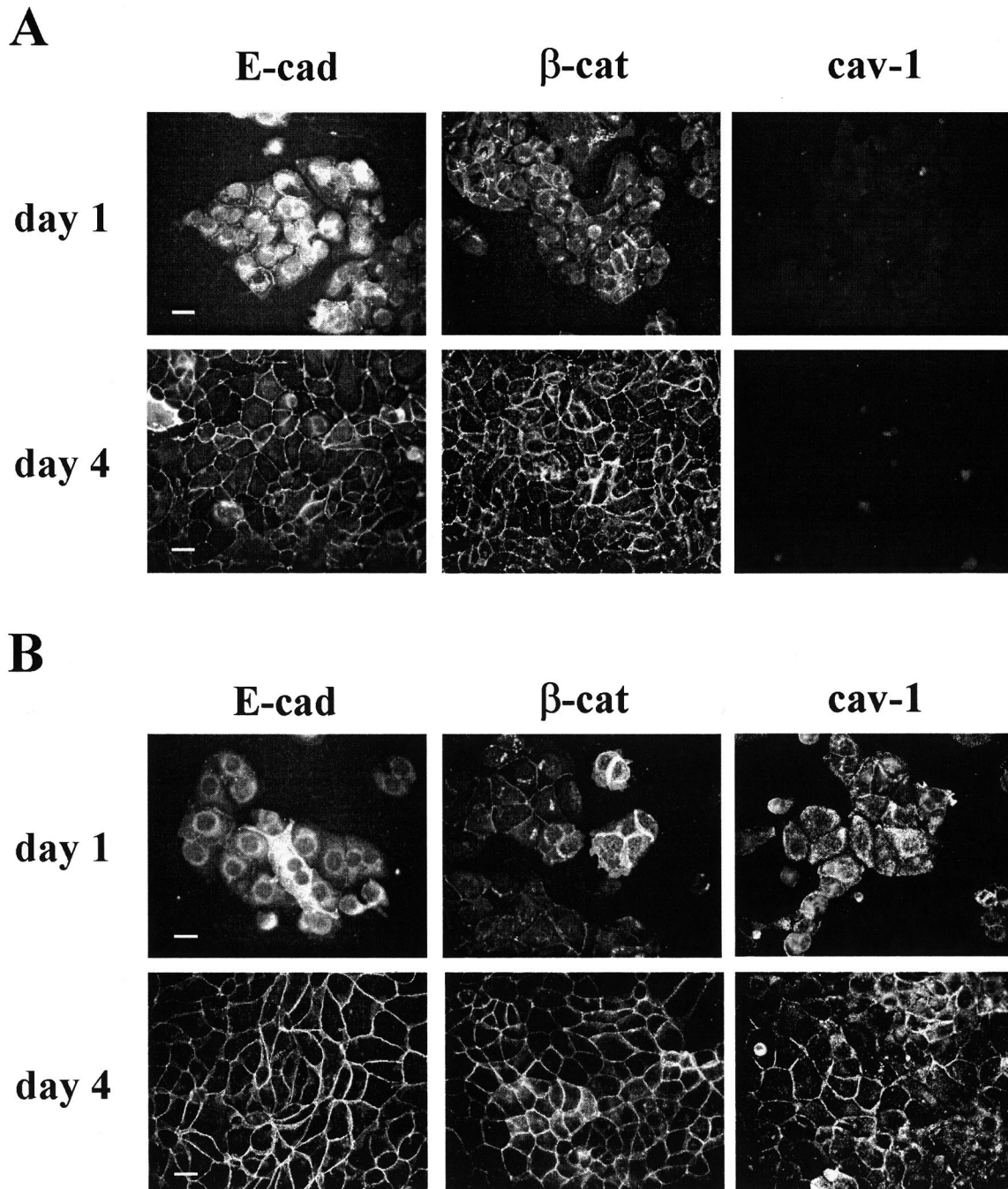


**Figure 3.** Morphological analysis reveals continuous cell-cell contacts only when cav-1 is expressed. IGtM87 (**A**) and IGtC3 (**B**) cells ( $3 \times 10^4$ /sample) were grown for 1 and 4 days on glass coverslips. After fixing in cold methanol, immunofluorescence staining was carried out using the relevant primary antibodies and fluoresceinated secondary antibodies. Early association of  $\beta$ -cat at cell-cell contacts takes place in cells of both lines (day 1), whereas at day 4 E-cad,  $\beta$ -cat, and cav-1 co-distributed at cell junctions. Epi-fluorescence images. Scale bar = 50  $\mu$ m.

cellularly, whereas  $\beta$ -cat was already localized at the cell junctions in both cell lines at 24 hours after seeding. At confluence (96 hours), both E-cad and  $\beta$ -cat were detected at the cell-cell contacts. In cav-1-negative IGtM87 cells, both E-cad and  $\beta$ -cat staining were irregular and discontinuous (Figure 3A) suggesting an active remodeling of cell junctions. In IGtC3 cells at 24 hours after seeding, cav-1 appeared to be diffusely distributed throughout the cell body, whereas at confluence (96 hours), cav-1 localized at the cell border together with

E-cad and  $\beta$ -cat so that the cell-cell contacts appeared more continuous (Figure 3B).

Lipid rafts are membrane microdomains enriched in cholesterol and glycosphingolipids and the site of a variety of signaling proteins. These microdomains serve as a potential platform for intracellular signaling.<sup>1,31</sup> Analysis of lipid rafts separated by sucrose gradient centrifugation of 1% TX-100 cell lysates showed that cav-1 was equally distributed in low-density top fractions (lipid rafts) and high-density bottom fractions in IGtC3 cells (Figure 4A)

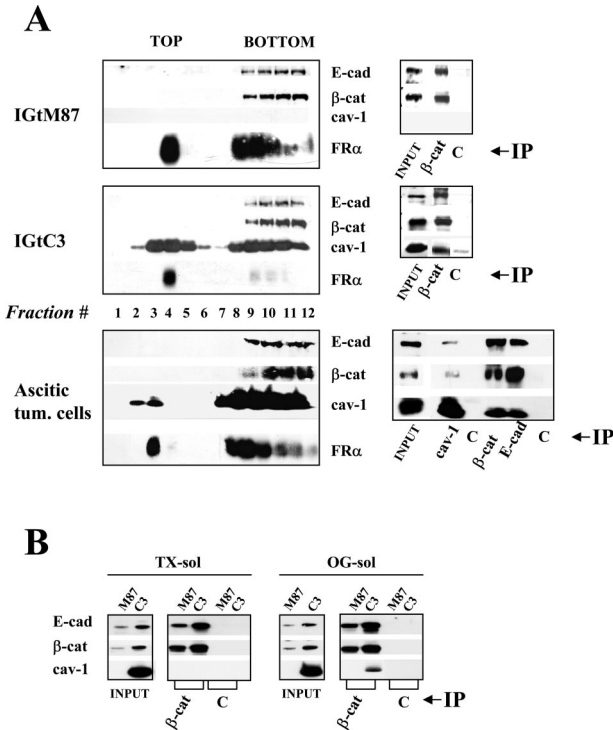


**Figure 4.** Biochemical characterization identifies E-cad/β-cat complexes containing cav-1. **A:** Lipid raft separation was carried on 1% TX-100 cell lysates of IGtM87 and IGtC3 cells and of ascitic tumor cells from an ovary carcinoma patient by flotation on a linear 5 to 30% sucrose gradient. After ultracentrifugation, recovered fractions were analyzed by SDS-PAGE and Western blotting; in none of the samples analyzed did E-cad and β-cat distribute in the top fractions of the gradient. The GPI-anchored protein folate receptor (FRα) was used as a marker of lipid rafts. Immunoprecipitation experiments show co-immunoprecipitation of soluble cav-1 with E-cad/β-cat complexes present in the bottom fractions of the gradient. **B:** Again, E-cad/β-cat complexes containing cav-1 were identified in the cytoskeleton-linked TX-100 insol/OG sol fraction obtained after milder 0.5% TX-100 treatment. To obtain these fractions, confluent cells were incubated in PBS+ for 1 hour at room temperature, and cell lysis (0.5% TX-100; 10 minutes, 4°C) was carried out in a flask with slight agitation. After recovery of solubilized proteins (TX-sol), further extraction was carried out for 30 minutes at 4°C in the same volume of buffer containing 1.1% OG, and the supernatant (TX-insol/OG-sol) was recovered by centrifugation.

and mainly in the bottom fractions in ascitic cells derived from an ovary carcinoma patient, for whom preliminary FACS analysis indicated the expression of cav-1, E-cad, and β-cat. Irrespective of cav-1 expression, E-cad and β-cat distributed only in the bottom fractions in all of the cells tested. Immunoprecipitation carried out on bottom fractions indicated reciprocal co-immunoprecipitation of the three molecules in IGtC3 and ascitic cells and co-precipitation of E-cad and β-cat in IGtM87 cells even in the absence of cav-1 (Figure 4A).

E-cad/β-cat complexes, which interact with the cytoskeleton,<sup>32</sup> are resistant to brief 0.5% TX-100 treatment after stabilization of cell-cell contacts in the presence of Ca<sup>2+</sup>. Co-immunoprecipitation experiments indicated recovery of E-cad/β-cat both from TX-sol and TX-insol/OG-sol fractions of IGtM87 and IGtC3 cells (Figure 4B). In IGtC3 cells, cav-1 co-immunoprecipitated with β-cat essentially in the OG-sol.

Together, these results suggest that all three molecules localize at the cell-cell contacts in confluent ovarian carcinoma cells. E-cad/β-cat complexes in either cav-1-

positive or -negative cells are not associated with conventionally defined lipid rafts, and complexes are formed between cav-1 and adherens junction proteins that can be recovered by immunoprecipitation of both the 1% TX-sol fraction and the cytoskeleton-linked 0.5% TX-insol/OG-sol fraction. The relatively low amount of cav-1 observed in the immunoprecipitates suggests that adherens junction molecules represent a minor fraction in the molecular complexes associated with cav-1. Thus, the presence of cav-1 might affect adherens junctions only indirectly.

### *Cav-1 Has Focal Contacts with β-cat and E-cad in Epithelial Ovarian Cells*

The cellular distribution of cav-1 and adherens junction proteins was initially investigated in IGtC3, MDCKII, and OSE cells (Figure 5). Confluent IGtC3 cells were double-stained with anti-cav-1 and anti-E-cad or anti-β-cat antibodies and analyzed by confocal microscopy in comparison with the MDCK II reference cell line. In agreement with a previous study,<sup>15</sup> cav-1 was present in MDCKII cells as a double layer of molecules distributed along the cell perimeter, and β-cat was distributed in the middle, with multiple points of co-localization between the two molecules. By contrast, cav-1 in IGtC3 cells displays few focal points of co-localization with E-cad and β-cat. Instead, cav-1 distributed at the cell border forming a line more or less parallel to proteins of the junctional complexes. In OSE cultured *in vitro* at early passage, cav-1 was found to accumulate at one cell side, from which spikes containing β-cat protruded, but not at the cell-cell contacts. By contrast, β-cat accumulated at the cell-cell contacts co-localized with α-cat (data not shown).

When we tested IGtC3 and IGtM87 cells for the co-localization of β-cat with E-cad at the cell-cell contacts (Figure 6), the cav-1-positive IGtC3 cells displayed a strict association of E-cad to the cell membrane and a continuous distribution of β-cat at the cell-cell contacts, whereas cav-1-negative IGtM87 cells were characterized by irregular/discontinuous membrane staining of the two proteins.

To evaluate the consequence of cav-1 down-regulation in IGtC3 cells, cav-1 was silenced using cav-1-specific siRNA oligonucleotides. Western blot analysis demonstrated the specific down-regulation of the relevant molecule (Figure 6B, bottom panel). Epi-fluorescence and confocal analysis showed that the reduction of cav-1 expression was accompanied by the formation of intracellular E-cad vesicles, suggestive of active adherens junction modulation.

### *Expression of cav-1 in Ovarian Carcinoma Cells Affects the Remodeling of Adherens Junctions*

Activated src kinases destabilize adherens junctions.<sup>33,34</sup> We found active src kinases in IGROV1 cells, expressing or not expressing cav-1, which are mainly



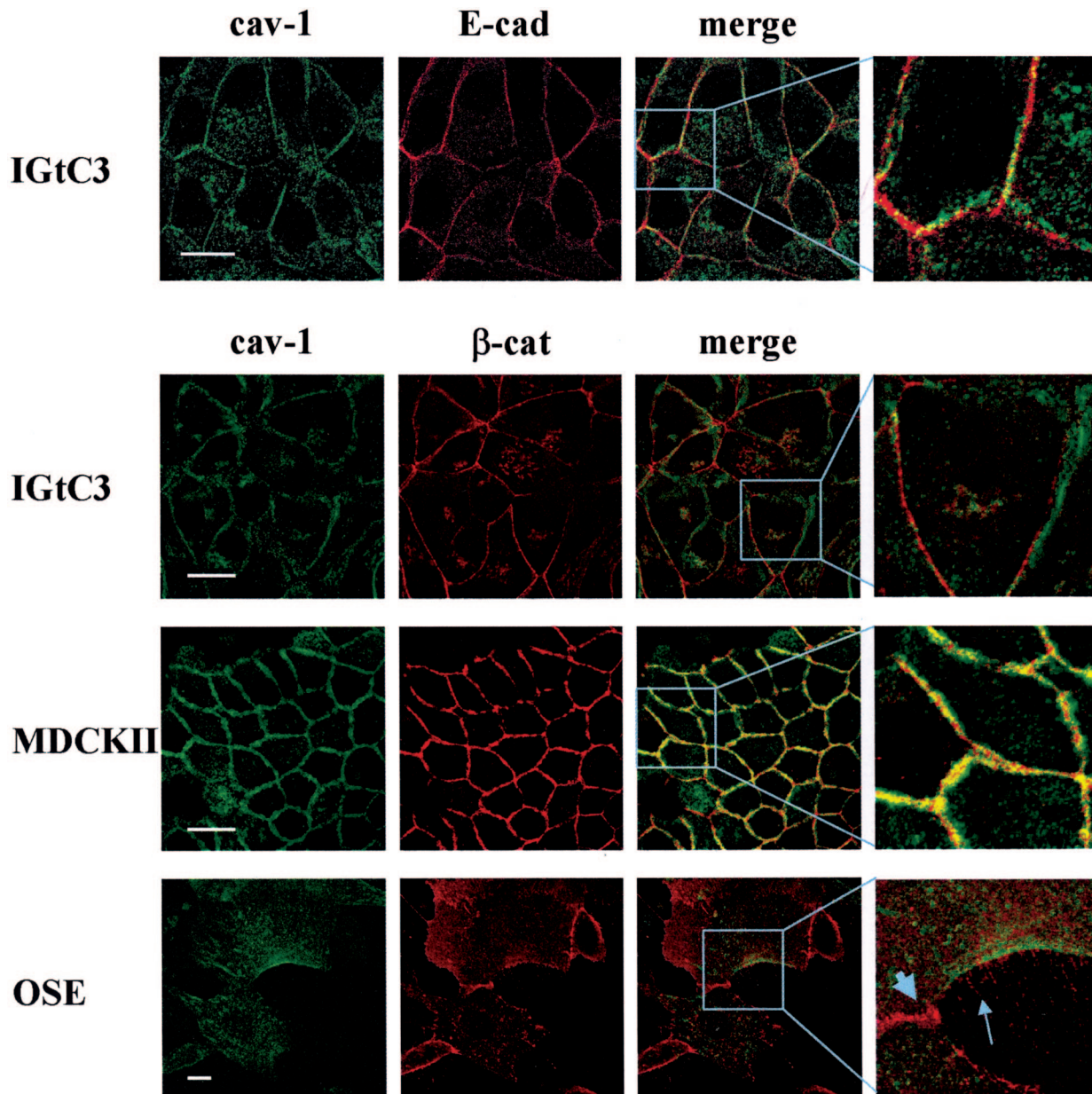


**Figure 5.** Cav-1 has focal contacts with  $\beta$ -cat and E-cad in ovarian epithelial cells. Confocal analysis was performed on methanol-fixed confluent cells stained with anti-E-cad,  $\beta$ -cat, and -cav-1 primary antibodies, as indicated in the figure. Strict colocalization between cav-1 and  $\beta$ -cat is observed in MDCKII cells, whereas few points of contact appear to exist between cav-1 and E-cad or  $\beta$ -cat in IGtC3 cells, suggesting that cav-1 contributes minimally to the formation of adherens junctions. In normal OSE, cav-1 accumulates at one cell side from which  $\beta$ -cat spikes protrude from the cell membrane and is completely excluded from the cell contacts. In the merge image of OSE cells, the **large arrow** and the **small arrow** indicate  $\beta$ -cat at the adherens junctions and  $\beta$ -cat spikes, respectively. Scale bar = 20  $\mu$ m.

associated with the TX-insol/OG-sol fraction (Figure 7A, bottom panel). Because the antibody we used recognizes several src family members in the active form, several bands were detected, in which intensity and pattern is different in the two cells and slightly less intense in IGtC3 than in IGtM87 cells. We tested the possible involvement of src kinases in the remodeling of cell-cell contacts of cav-1-expressing or -nonexpressing IGROV1 cells using the specific src kinase inhibitor PP1.<sup>35</sup> Tyrosine phosphorylation of TX-sol and TX-insol/OG-sol proteins decreased in a dose-dependent manner. In particular, proteins in the 50- to 60-kd range, which corre-

sponds to the size of src family proteins, were less phosphorylated (Figure 7A, top panel). At all PP1 doses, treated IGtM87 cells displayed increased levels of E-cad, whereas IGtC3 cells showed a slight but much smaller increase in E-cad expression than in IGtM87 cells at the intermediate dose of PP1.  $\beta$ -cat levels remained essentially stable in both cell lines (Figure 7B). At the PP1 intermediate dose, 4  $\mu$ mol/L, a reduction of the src family kinases active form was confirmed in both the cells, particularly in the OG-sol fraction (Figure 7A, bottom panel), and similarly a 40% reduction in cell proliferation was detected both in IGtM87 and IGtC3 cells (data not

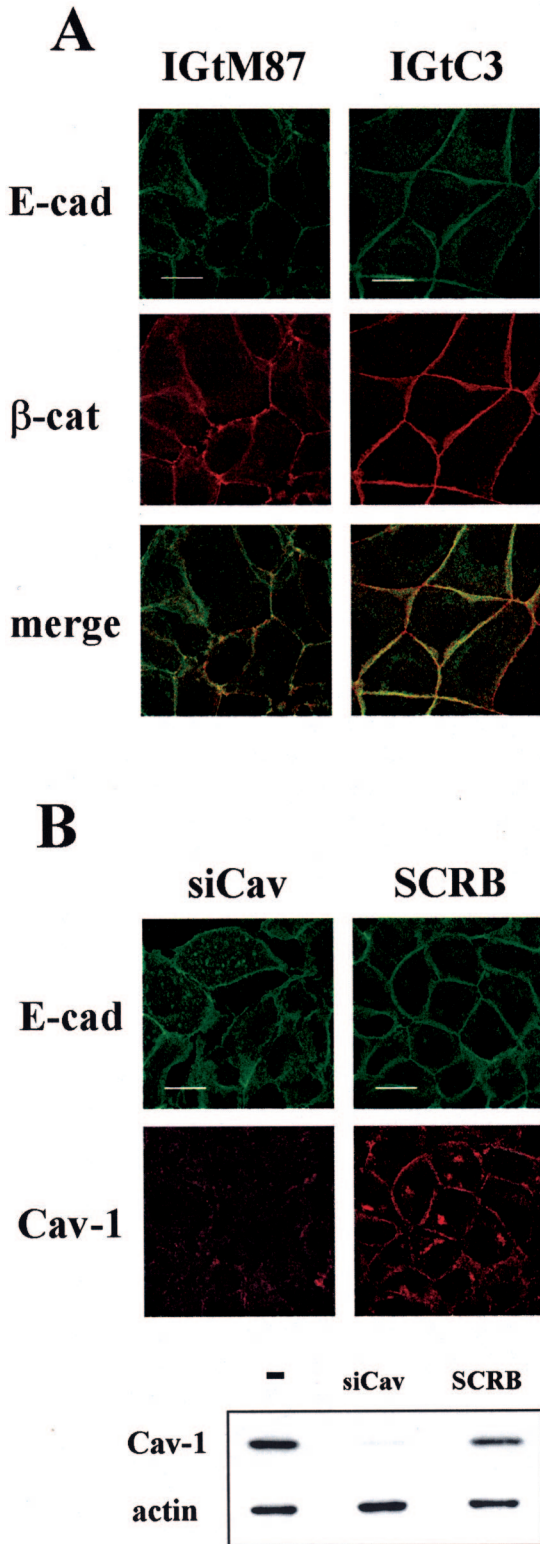


**Figure 6.** Cav-1-positive ovarian carcinoma cells show E-cad only at cell-cell contacts. **A:** Confluent IGtM87 and IGtC3, grown on glass coverslips, were fixed in cold methanol and double-stained with anti-E-cad and anti-β-cat and secondary fluoresceinated antibodies. Cav-1-positive cells display a strict association of E-cad to the cell membrane where it co-localizes with β-cat, whereas cav-1-negative IGtM87 cells are characterized by irregular/discontinuous membrane staining of adherens junction proteins. **B:** Silencing of cav-1 by siRNA, documented by Western blot analysis (**bottom panel**), resulted in formation of intracellular E-cad vesicles not present in control-treated (SCRb) cells. Color images were obtained by confocal microscopy. Scale bar = 20 μm.

show). Because higher doses were found to affect cell viability, 4 μmol/L PP1 dose was used in further experiments. As shown by epi-fluorescence analysis, E-cad staining intensity increased and became more continuous in IGtM87 cells treated with this dose of drug (Figure 7C). Staining intensity was also increased in IGtC3 cells. In both cell lines, a deeper distribution of E-cad reaching the ventral face of the cells was observed (not shown).

Decreases in extracellular Ca<sup>2+</sup> concentrations to the micromolar range disrupt the intercellular junctions of epithelial cells, inducing rapid internalization of the junctional complexes.<sup>36,37</sup> Both IGtM87 and IGtC3 cells maintained cell-cell and cell-substrate adhesion at high millimolar Ca<sup>2+</sup> concentrations irrespective of PP1 treatment (Figure 8). IGtM87 cells were highly sensitive to Ca<sup>2+</sup> depletion, with consequent cell rounding, E-cad punctuate staining, and substrate detachment; PP1 treatment only partially reversed cell-cell adhesion (Figure 8A, left). By contrast, IGtC3 cells showed modest cell rounding and cytoplasmic E-cad redistribution during incubation with low Ca<sup>2+</sup> concentrations, and both effects were inhibited by culturing the cells with PP1 (Figure 8A, right). These data further suggest that the presence of cav-1 is a determining factor of both cell-cell and cell-substrate adhesion. Cell-substrate adhesion assay of IGtM87 and IGtC3 cells seeded on plastic (Figure 8B) revealed reproducibly higher levels of substrate adhesion in IGtC3 cells than in cav-1-negative IGtM87 cells at either 1 or 2 hours after seeding.

#### *Cav-1 and/or PP1 Treatment Relocalizes p120ctn to the Cell Membrane of Ovarian Carcinoma Cells*

The catenin p120 (p120ctn) binds E-cad in the juxtamembrane position and is a known target of src kinase activity.<sup>22,38</sup> Epi-fluorescence analysis of p120ctn distribution (Figure 9A) revealed irregular membrane staining with intense cytoplasmic, particularly perinuclear, localization of the protein in IGtM87 cells, whereas in cav-1-positive IGtC3 cells, p120ctn was mainly membrane associated. The differential p120ctn distribution in the two cell lines was confirmed by biochemical subcellular fractionation (Figure 9B), which shows the protein mostly in the cytoplasmic fraction in IGtM87 cells, but mostly membrane associated in cav-1-positive IGtC3 cells. The p120ctn protein is expressed by both IGtM87 and IGtC3 cells as different shared isoforms, with bands ranging from 104 to 64 kd. No expression of the 120-kd-longer isoform 1, characteristic of fibroblast and highly motile cells, was detected in both cells (Figure 9, B and C). All of the expressed isoforms are mainly present in the TX-sol fraction, whereas in the OG-sol fraction distributed only a minor amount of the two higher molecular weight bands. E-cad appeared to be present only in the membrane fraction in both cell lines, even though expression level is different. Immunoprecipitation experiments using an anti-E-cad antibody to evaluate the association of E-cad with p120ctn revealed E-cad/

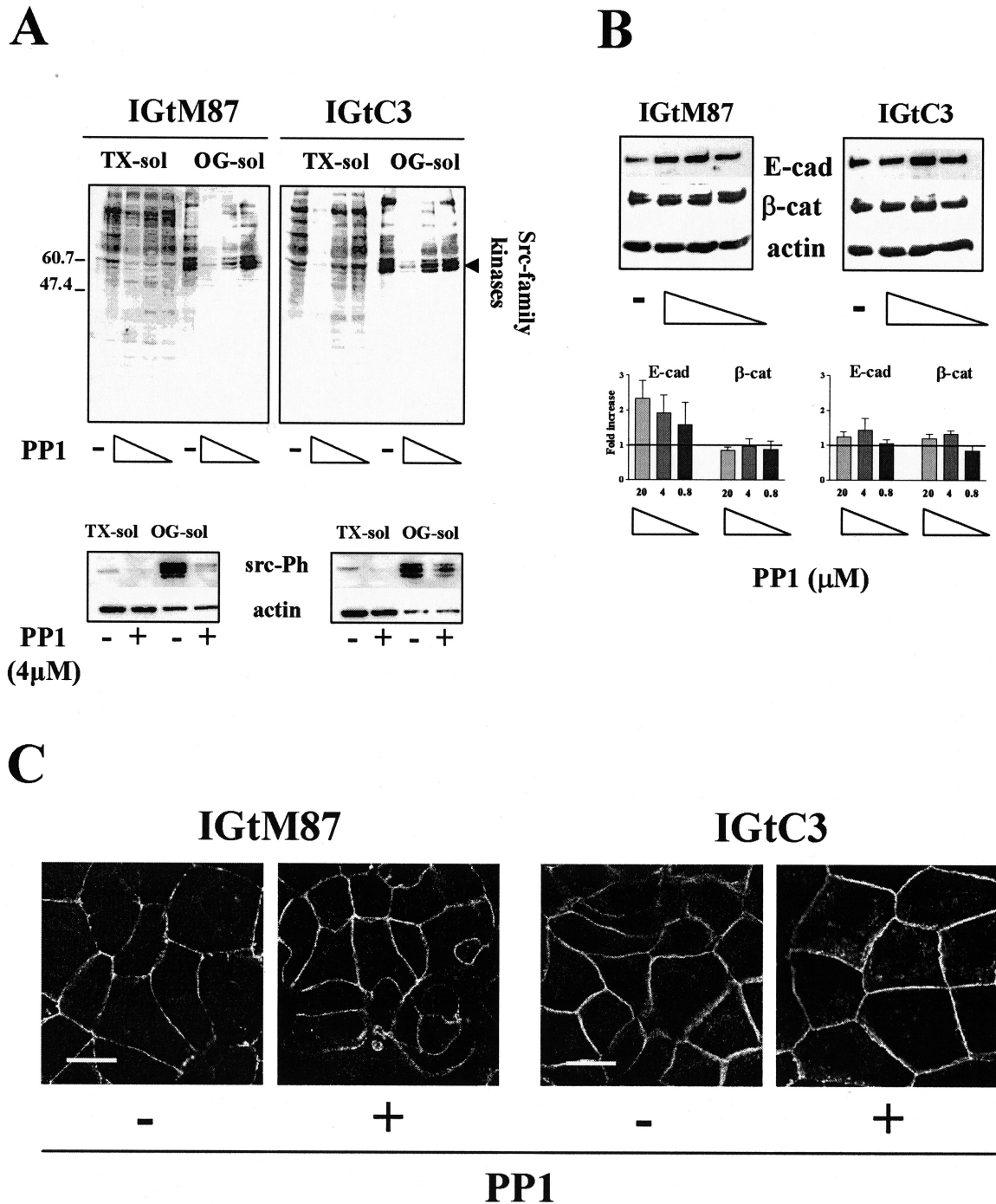


**Figure 7.** The src kinase inhibitor PP1 restores cell-cell contacts of cav-1-negative ovarian carcinoma cells by increasing E-cad expression. Cells were grown for 3 days before medium containing the src inhibitor PP1 (20, 4, and 0.8  $\mu$ mol/L) or DMSO-containing control medium was added and cultures continued for another 2 days. Cells were submitted to mild TX-100 solubilization. **A:** Dose-dependent reduction of tyrosine phosphorylation, particularly in the 50- to 60-kd range, which corresponds to src family kinases (**top panel**). Rabbit anti-src pY418 (**bottom panel**) revealed the presence of active src family kinases concentrated in the OG-sol fraction of both of the cells. Reactivity, slightly higher in IGtM87 cells, was sensitive to 4  $\mu$ mol/L PP1 treatment in both cells. **B:** PP1 treatment induced a dose-dependent increase in E-cad expression, particularly in IGtM87 cells. Samples analyzed by Western blot derive from the pool of TX-sol and TX-insol/OG-sol fraction (30  $\mu$ g). Results of a representative experiment together with densitometric evaluation of the fold increase (mean  $\pm$  SD of three separate experiments) are shown. Each value used to calculate the ratio between treated and untreated cells was normalized to the respective  $\beta$ -actin expression level. **C:** Confocal analysis of relevant cells before and after 4  $\mu$ mol/L PP1 treatment shows increased and more continuous and regular E-cad distribution at the cell-cell contacts in PP1-treated cells. Scale bar = 20  $\mu$ m.

p120ctn complexes mainly immunoprecipitated in the OG-sol fraction of cav-1-positive IGtC3 cells. Complexes were less evident in the immunoprecipitate of IGtM87 cells (Figure 9B, bottom panel). Inhibition of src

kinase activity with 4  $\mu$ mol/L PP1, reduced the phosphorylation of higher molecular weight p120ctn isoforms (range, 104 to 90 kd), particularly those present in the OG-sol fraction in both cells lines (Figure 9C). As



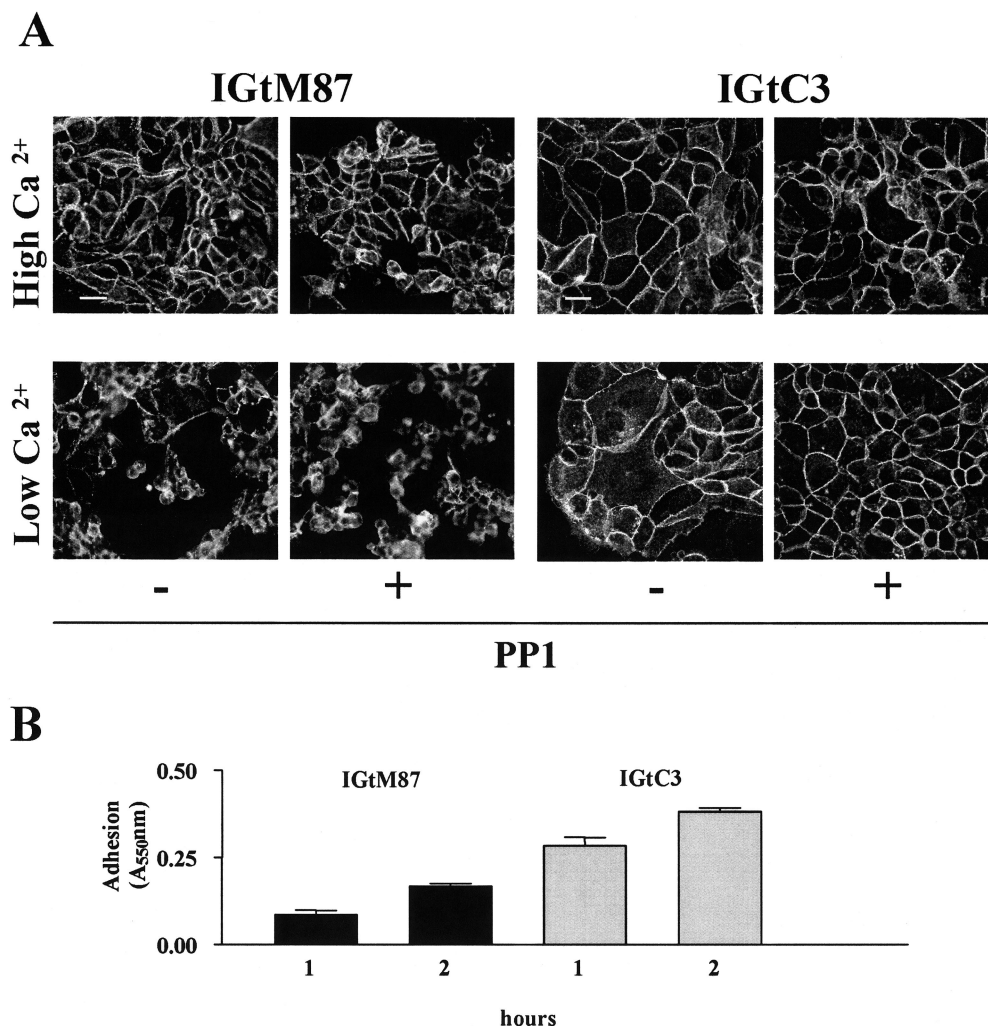


**Figure 8.** Ca<sup>2+</sup>-dependent cell adhesion is stronger in cav-1-positive cells and is further stabilized by the src kinase inhibitor PP1. **A:** Cells were grown on glass coverslips for 3 days and treated with 4  $\mu$ mol/L PP1 or DMSO-containing medium for 2 more days. After removal of culture medium, cells were incubated for 90 minutes at 37°C in the presence of PBS containing high (1 mmol/L) or low (0.030 mmol/L) Ca<sup>2+</sup> concentrations, fixed in cold methanol, and immunostained for E-cad as in Figure 3. IGtM87 cells were much more sensitive than cav-1-positive cells to Ca<sup>2+</sup> depletion, affecting both cell-cell and cell-substrate adhesion. Whereas in IGtC3 cells, both the effects were completely inhibited by PP1 treatment, only cell-cell adhesion was inhibited, and only partially in IGtM87 cells. Scale bar = 50  $\mu$ m. **B:** Substrate adhesion evaluated on plastic at different times. Cav-1-positive IGtC3 cells showed more extensive adherence to substrate than did cav-1-negative IGtM87 cells. The graphic reports the mean of three replicates  $\pm$  SD of one experiment representative of three.

a consequence of PP1 treatment, in IGtM87 cells, the protein was found to relocate to the plasma membrane in sites corresponding to cell-cell contacts; no dramatic changes were observed in PP1-treated IGtC3 cells (Figure 9C, bottom panel). These results further support a role for cav-1 in the organization of adherens junction proteins at the membrane level.

#### *Cav-1/Adherens Junction Protein Relationship in SKOV3 Ovarian Carcinoma Cells*

SKOV3 cells express high levels of cav-1,<sup>5</sup> consistent with findings in some ovarian carcinoma specimens as shown in Figure 1A. This cell line represents an interesting model because in epi-fluorescence analysis, cells appear homogeneously cav-1-positive but display a heterogeneous E-cad staining. Groups of cell frankly E-cad positive are characterized by membrane

distribution of the protein. The presence of E-cad at the cell-cell contacts appears to correlate with the membrane distribution of  $\beta$ -catenin and p120ctn and also the localization of cav-1 (Figure 10A). Cav-1 localizes at the cell-cell contacts only in SKOV3 cells that evidence E-cad on the membrane. Inhibition of src kinases by PP1 in SKOV3 cells induced the up-modulation of E-cad expression (Figure 10B left) and the membrane relocation of both E-cad and p120ctn as evaluated by epi-fluorescence (Figure 10B, right). E-cad modulation was PP1 dose dependent and inversely related to src phosphorylation inhibition (Figure 10B, left). Silencing of cav-1 in SKOV3 cells (Figure 10C) led a 70% reduction of cav-1 expression (Figure 10C, left panel) and a more evident intracellular distribution of E-cad (Figure 10C, right panel), although some protein remained membrane associated.

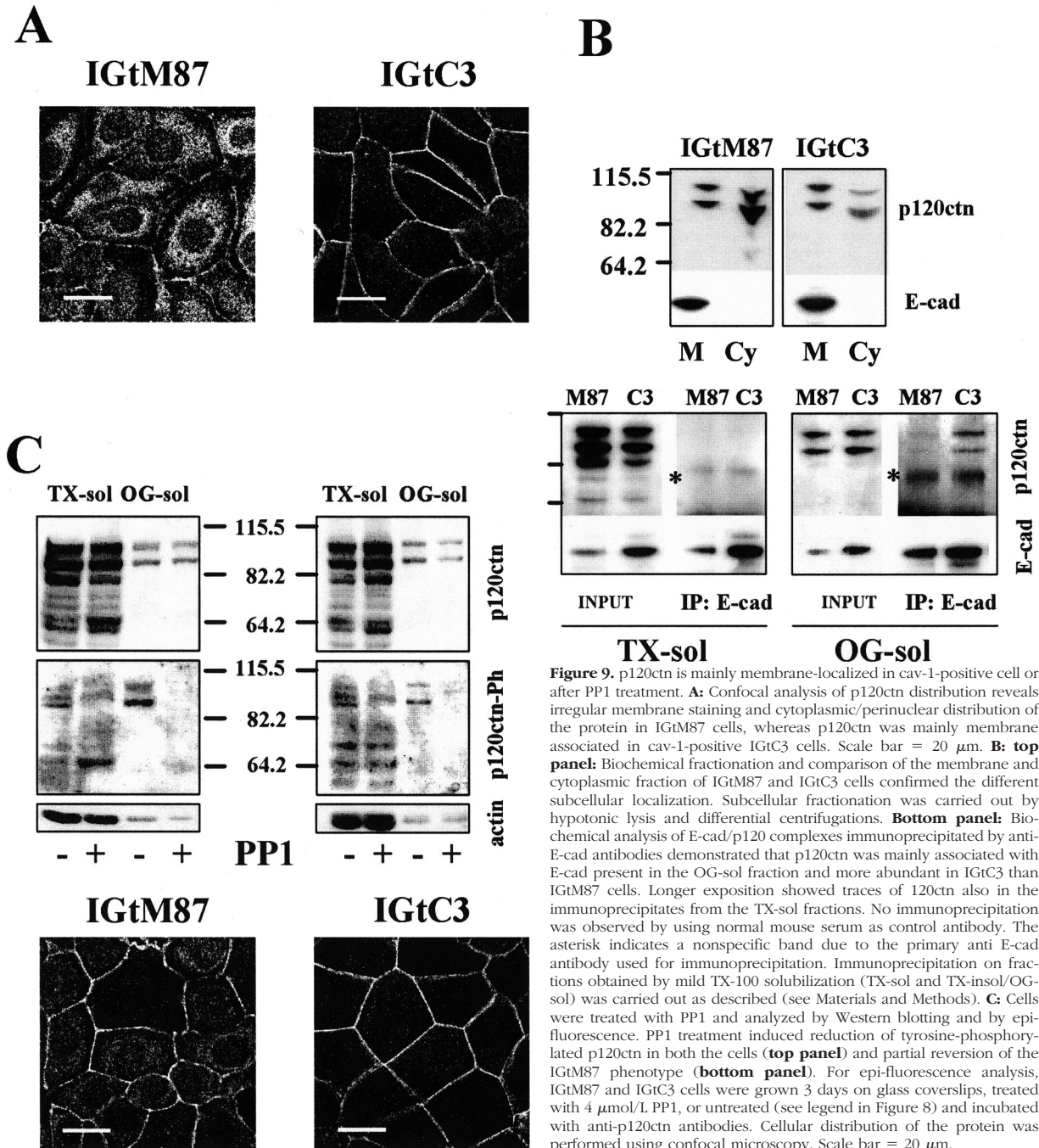
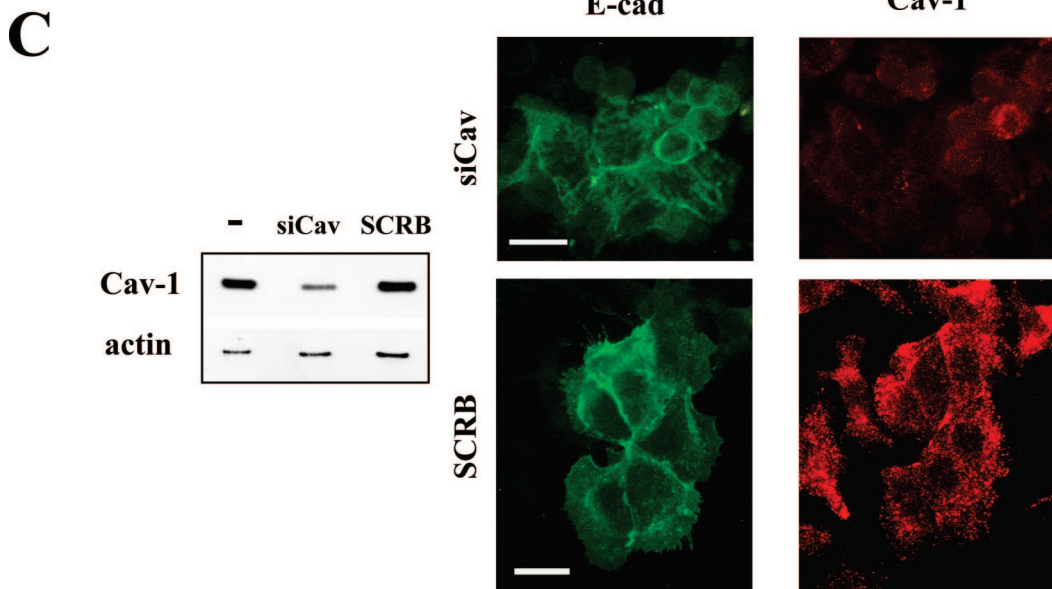
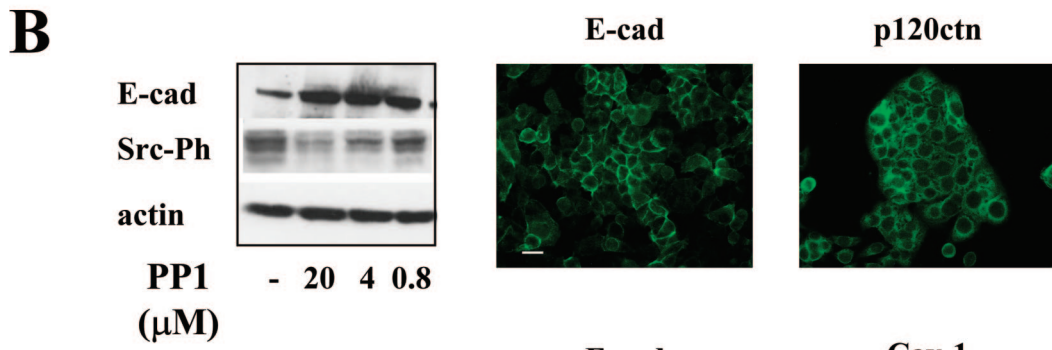
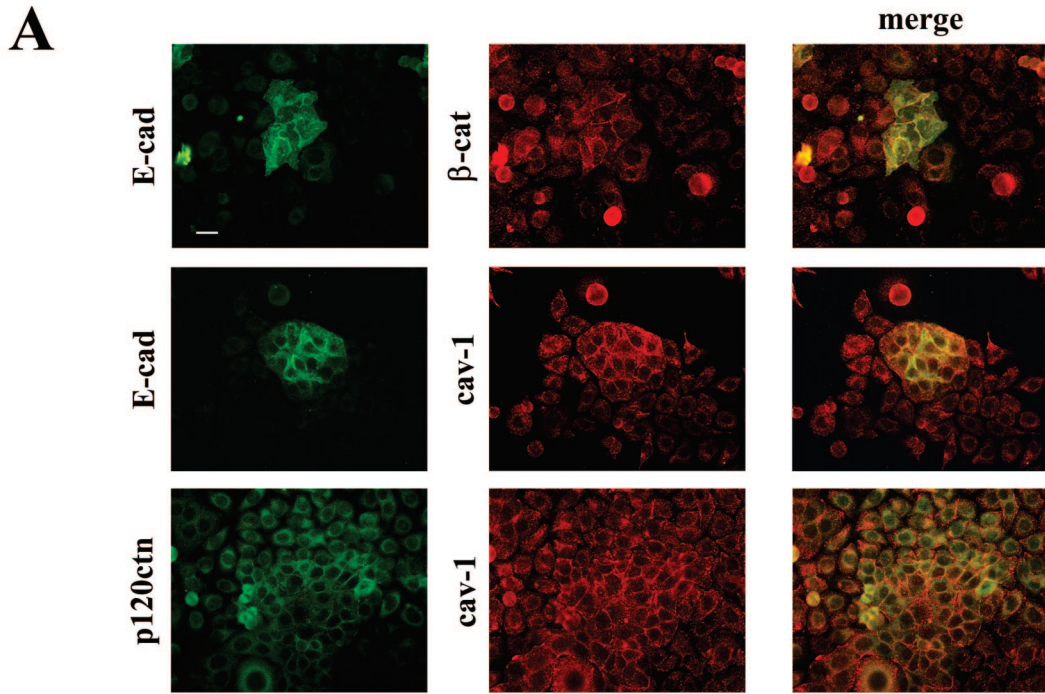


**Figure 9.** p120ctn is mainly membrane-localized in cav-1-positive cell or after PP1 treatment. **A:** Confocal analysis of p120ctn distribution reveals irregular membrane staining and cytoplasmic/perinuclear distribution of the protein in IGtM87 cells, whereas p120ctn was mainly membrane associated in cav-1-positive IGtC3 cells. Scale bar = 20  $\mu$ m. **B: top panel:** Biochemical fractionation and comparison of the membrane and cytoplasmic fraction of IGtM87 and IGtC3 cells confirmed the different subcellular localization. Subcellular fractionation was carried out by hypotonic lysis and differential centrifugations. **Bottom panel:** Biochemical analysis of E-cad/p120 complexes immunoprecipitated by anti-E-cad antibodies demonstrated that p120ctn was mainly associated with E-cad present in the OG-sol fraction and more abundant in IGtC3 than IGtM87 cells. Longer exposition showed traces of p120ctn also in the immunoprecipitates from the TX-sol fractions. No immunoprecipitation was observed by using normal mouse serum as control antibody. The asterisk indicates a nonspecific band due to the primary anti E-cad antibody used for immunoprecipitation. Immunoprecipitation on fractions obtained by mild TX-100 solubilization (TX-sol and TX-insol/OG-sol) was carried out as described (see Materials and Methods). **C:** Cells were treated with PP1 and analyzed by Western blotting and by epi-fluorescence. PP1 treatment induced reduction of tyrosine-phosphorylated p120ctn in both the cells (**top panel**) and partial reversion of the IGtM87 phenotype (**bottom panel**). For epi-fluorescence analysis, IGtM87 and IGtC3 cells were grown 3 days on glass coverslips, treated with 4  $\mu$ mol/L PP1, or untreated (see legend in Figure 8) and incubated with anti-p120ctn antibodies. Cellular distribution of the protein was performed using confocal microscopy. Scale bar = 20  $\mu$ m.

### Discussion

The functional role of cav-1 in tumor development and progression is under investigation in various experimental models of breast carcinoma, in which cav-1 expression appears to inhibit *in vivo* tumor growth and metastasis development.<sup>11,39–41</sup> We and others reported down-regulation of cav-1 expression in ovarian carcinomas,<sup>5,10,42</sup> but the biological significance of this down-regulation in the ovarian context has not been widely investigated. In the present study, we focused on the effects of cav-1 down-regulation on cell-cell interactions mediated by the E-cad/ $\beta$ -cat system using an experimen-

tal model of ovarian tumor cells transfected with cav-1.<sup>5</sup> Our data suggest that, when ectopically restored in ovarian carcinoma cells (IGtC3), cav-1 contributes to the organization and stability of adherens junctions through an increase in E-cad expression and increased association of E-cad and p120ctn at the junctional level. Because comparable effects were observed in cav-1-negative cells (IGtM87) after pharmacological inhibition of src kinase activity and in an ovarian carcinoma cell line endogenously expressing cav-1, we suggest that cav-1 indirectly modulate adherens junctions through the inhibition of src-related kinases.





The normal human ovary is characterized by the presence of a monolayered simple epithelium (OSE) that, unlike other more differentiated epithelia, is loosely attached to its basement membrane.<sup>43</sup> OSE cells display polarized baso-lateral expression of cav-1,<sup>5,10</sup> suggesting a role for the protein in mediating cell-substrate and/or cell-cell interactions; however, OSE cells do not express E-cad.<sup>43</sup> Neo-expression of E-cad is part of the Mullerian-like differentiation of OSE cells, which takes place in the normal ovary in sites corresponding with surface invaginations and inclusion cysts, considered to be precursors of epithelial ovarian tumors.<sup>43,44</sup> During these very early OSE modifications, we found that E-cad neo-expression coincided with the loss of cav-1 expression, suggesting that the two genes respond inversely to factors that modify gene expression in premalignant ovary epithelium.

Lu et al<sup>19</sup> recently proposed a model of constitutive EGF-induced internalization of E-cad and cav-1 in caveolae, leading to stable transcriptional down-regulation of both E-cad and cav-1 and activation of the  $\beta$ -cat signaling pathway in tumor cells; however, the peculiar characteristics of ovarian epithelium together with our present findings, argue against the applicability of that model to ovarian carcinomas. Moreover, we found only negligible  $\beta$ -cat transcriptional activity in IGROV1 cells, irrespective of cav-1 transfection, and that cav-1 expression did not enhance the recruitment of  $\beta$ -cat to the cell membrane of IGtC3 cells, with a corresponding decrease in the nuclear fraction, as reported in other cell systems.<sup>18</sup> These results are in accord with data indicating that activation of the  $\beta$ -cat/TCF pathway is rare in ovarian cancer cell lines.<sup>45</sup>

Our microscopy analysis identified cav-1 in sites corresponding to cell-cell contacts, where E-cad/ $\beta$ -cat complexes are also found. Our collective data, including co-immunoprecipitation experiments, indicate a limited interaction between cav-1 and adherens junction molecules. No association of E-cad/ $\beta$ -cat with caveolae/lipid rafts was revealed in the cav-1-transfected IGROV1 model or in cells derived from ascite of an ovary carcinoma patient. Other studies have reported that polarized epithelial cells, such as MDCKII (from dog normal kidney)<sup>18</sup> and T84 (from human columnar intestine),<sup>46</sup> are positive and negative, respectively, for association of adherens junction proteins with caveolae. TX-insol/OG-sol E-cad/ $\beta$ -cat complexes, which are thought to be responsible for stable cell-cell *trans*-interactions and cytoskeletal connection, could be sites for interaction with cav-1. Confocal microscopy analysis of the cellular distribution of cav-1 in relation to that of adherens junction proteins provided experimental proof that the two molecular complexes in IGtC3 cells are distinct, with only focal points of contact. By contrast, MDCKII cells evidenced

co-localization of cav-1 and  $\beta$ -cat. The cell type-dependent distribution of cav-1 and  $\beta$ -cat was even more evident in normal OSE cells, where cav-1 did not co-localize with  $\beta$ -cat at the cell-cell contacts but was distributed where spikes of  $\beta$ -cat protrude from the plasma membrane. Together, these data suggest that cell context can be relevant in dictating an association of E-cad/ $\beta$ -cat complexes to membrane microdomains.

Both the membrane and intracellular distribution of E-cad in ovarian carcinoma have been reported,<sup>24,25</sup> suggesting that even if protein expression is transcriptionally maintained, posttranslational mechanisms, such as activated src kinases, might modulate E-cad expression and functionality. We did not have evidence of great differences in total src kinase activity between IGtM87 and IGtC3 cell, but it is known that src kinases can induce the remodeling of adherens junctions at multiple levels: 1) src-mediated phosphorylation of adherens junction components such as  $\beta$ -cat and p120ctn reduces their interaction with E-cad;<sup>20</sup> 2) endocytosis of E-cad/ $\beta$ -cat is regulated through src-mediated tyrosine phosphorylation of Hakai, a Cbl-like E3-ubiquitin ligase that ubiquitinates E-cad and  $\beta$ -cat, leading to their internalization;<sup>47</sup> 3) activated src perturbs the activity of Arf6GTPase, which controls the translocation of E-cad from membrane to intracellular compartments;<sup>48</sup> and 4) integrin-mediated cell-matrix interaction activates src kinases, deregulating E-cad-mediated cell-cell contacts.<sup>49</sup> Although our analysis of surgical specimens confirmed E-cad dual distribution, ie, membrane and/or intracellular, in cav-1-negative tumors, the membrane association of both E-cad and  $\beta$ -cat was pronounced in the few cases displaying polarized cav-1 expression at the tumor-stroma interface. In cav-1-negative IGtM87 cells, with fainter and discontinuous membrane plus intracellular E-cad staining compared with the cav-1-positive IGtC3 cells, analysis of subcellular fractionation revealed more cytoplasmic- than membrane-associated p120ctn. It has been reported that the p120ctn shorter isoforms preferentially interact with E-cad, whereas the longer isoform 1 interacts with N-cadherin.<sup>50</sup> Our immunoprecipitation experiments showed interaction of the two mainly expressed p120ctn isoforms to E-cad and confirmed that the association was higher in IGtC3 cells than in non-transfected cells. Because a similar pattern of phosphorylated isoforms is present in both IGtM87 and IGtC3 cells, the role of p120ctn phosphorylation status in these cells needs to be further investigated. Interestingly, a dual role for p120ctn as a function of its intracellular distribution has been hypothesized, ie, it acts as a tumor suppressor when bound to the cell membrane because it stabilizes E-cad complexes or, in the absence of E-cad, it accumulates in the cytoplasm and acts as a metastasis promoter through the inhibition of RhoA activity.<sup>51</sup> Furthermore, p120ctn nuclear localization might be an important factor in regulating

**Figure 10.** SKOV3 cells display membrane-associated cav-1 only in E-cad-expressing cells. **A:** Epi-fluorescence analysis of indicated proteins in methanol-fixed SKOV3 cells. E-cad conditions the membrane localization of cav-1 and also of  $\beta$ -cat and p120ctn. **B:** Cells were treated with PP1 and analyzed for E-cad expression and p120 distribution by epi-fluorescence (**right panel**) on methanol-fixed cells and Western blot (**left panel**) on total cell lysates. Inhibition of src kinase activity by PP1 had a strong effect on the induction of E-cad expression and relocalization of p120ctn at the cell membrane. Western blot with anti-src pY418 also shows the reduction of phosphorylation of src kinases, which demonstrate the efficacy of PP1 treatment. **C:** Silencing of cav-1 expression in SKOV3 cells by siRNA analyzed by epi-fluorescence (**right panel**) and Western blotting (**left panel**). Down-regulation of cav-1 expression induced an increased cytoplasmic distribution of E-cad. Western blot analysis on cell lysates of silenced and control cells (SCRB) confirmed the reduction of cav-1 expression. Scale bar in **A**, **B**, and **C** = 50  $\mu$ m.

genes associated with an invasive phenotype, such as MMP7, through binding to the transcriptional repressor KAISO.<sup>52</sup> Our data suggest that in ovarian carcinoma, cytoplasmic p120ctn might lead to weaker E-cad-mediated cell-cell interactions and easier cell detachment from the primary tumor. This hypothesis is consistent with data indicating that a cytoplasmic distribution of p120ctn concomitant with a loss of E-cad expression characterizes the invasive phenotype of lobular histotype in breast carcinoma.<sup>53</sup>

In addition to the IGROV1 model with transfected cav-1, we examined the SKOV3 cell line, which unlike most ovarian carcinoma cell lines, spontaneously expresses high levels of cav-1. This overexpression is not necessarily representative of a more normal phenotype, because overexpression of cav-1 in late-stage tumor has recently been associated with a more aggressive behavior. In SKOV3 cells (heterogeneously positive for E-cad and homogeneously positive for cav-1), the distribution of cav-1 at the cell-cell contacts follows the distribution of E-cad in those groups of cells clearly E-cad positive. The presence of E-cad at the cell-cell contacts appears to be a conditioning factor for membrane distribution of  $\beta$ -cat and p120ctn. Although we do not have a simple explanation for E-cad heterogeneous expression, we showed that the activity of src kinases in SKOV3 cells play a role in the reduction of E-cad expression, as demonstrated by pharmacological inhibition of their activity. It is also evident that the overexpressed cav-1 cannot control the activity of these kinases in most SKOV3 cells, except probably in the few E-cad-positive cells. In agreement with our hypothesis, in both IGtC3 and SKOV3 cells, the silencing of cav-1 leads to junction remodeling as observed in IGtM87 cells, with appearance in IGtC3 cells of E-cad-positive vesicles.

We previously reported the reduced number of non-adherent cells and the reduced anchorage-independent growth in IGROV1 cells after cav-1 transfection,<sup>42</sup> strongly suggesting a modified substrate interaction. Our adhesion assay in the present paper confirms that cav-1-positive cells display higher adhesive capability than IGtM87 cells. Using  $\text{Ca}^{2+}$  depletion and/or src kinase inhibition in cav-1-positive and -negative cells, we provided evidence that PP1 inhibits the src activity responsible for adherens junction remodeling in both cell lines, but in the absence of cav-1, it cannot reverse the effect of  $\text{Ca}^{2+}$  in decreasing both cell-cell and cell-substrate adhesion. These and other findings support the notion that cav-1 up-modulates adherens junctions possibly through substrate adhesion. Thus, cav-1 could represent an important molecule in the described src-mediated interplay between cadherin- and integrin-mediated adhesion.<sup>49,54</sup> This possibility merits exploration, awaiting further studies to define the molecules that physically and functionally link cav-1 to adherens junction complexes.

In conclusion, the simultaneous expression of cav-1 and E-cad, both of which are considered to play an onco-suppressive role, appears to be required in stabilizing adherens junction and substrate adhesion in ovarian carcinoma cells. The activation and/or overexpression of src family proteins have been described in a large fraction of human tumors<sup>55</sup> and also in the majority of late-stage ovarian carcinoma.<sup>56,57</sup> Alteration in src ki-

nases, together with a reduced expression of cav-1, which negatively regulates their activity,<sup>58</sup> might contribute significantly to the pathobiology of ovarian tumors by affecting the stability of adherens junctions and thereby the spread of tumor cells in the peritoneal cavity.

## Acknowledgments

We thank the clinical staff of Istituto Nazionale Tumori for providing the surgical specimens, Dr. Cristiano Rumio for help in confocal microscopy analysis, and Miss Gloria Bosco for secretarial assistance.

## References

- Galbiati F, Razani B, Lisanti MP: Emerging themes in lipid rafts and caveolae. *Cell* 2001, 106:403–411
- Liu P, Rudick M, Anderson RG: Multiple functions of caveolin-1. *J Biol Chem* 2002, 277:41295–41298
- Carver LA, Schnitzer JE: Caveolae: mining little caves for new cancer targets. *Nat Rev Cancer* 2003, 3:571–581
- Racine C, Belanger M, Hirabayashi H, Boucher M, Chakir J, Couet J: Reduction of caveolin 1 gene expression in lung carcinoma cell lines. *Biochem Biophys Res Commun* 1999, 255:580–586
- Bagnoli M, Tomassetti A, Figini M, Flati S, Dolo V, Canevari S, Miotti S: Downmodulation of caveolin-1 expression in human ovarian carcinoma is directly related to  $\alpha$ -folate receptor overexpression. *Oncogene* 2000, 19:4754–4763
- Bender FC, Reymond MA, Bron C, Quest AF: Caveolin-1 levels are down-regulated in human colon tumors, and ectopic expression of caveolin-1 in colon carcinoma cell lines reduces cell tumorigenicity. *Cancer Res* 2000, 60:5870–5878
- Razani B, Schlegel A, Liu J, Lisanti MP: Caveolin-1, a putative tumour suppressor gene. *Biochem Soc Trans* 2001, 29:494–499
- Wiechen K, Sers C, Agoulnik A, Arlt K, Dietel M, Schlag PM, Schneider U: Down-regulation of caveolin-1, a candidate tumor suppressor gene, in sarcomas. *Am J Pathol* 2001, 158:833–839
- Aldred MA, Ginn-Pease ME, Morrison CD, Popkie AP, Gimm O, Hoang-Vu C, Krause U, Dralle H, Jhiang SM, Plass C, Eng C: Caveolin-1 and caveolin-2, together with three bone morphogenetic protein-related genes, may encode novel tumor suppressors down-regulated in sporadic follicular thyroid carcinogenesis. *Cancer Res* 2003, 63:2864–2871
- Wiechen K, Diatchenko L, Agoulnik A, Scharff KM, Schober H, Arlt K, Zhumabayeva B, Siebert PD, Dietel M, Schafer R, Sers C: Caveolin-1 is down-regulated in human ovarian carcinoma and acts as a candidate tumor suppressor gene. *Am J Pathol* 2001, 159:1635–1643
- Williams TM, Cheung MW, Park DS, Razani B, Cohen AW, Muller WJ, Di Vizio D, Chopra NG, Pestell RG, Lisanti MP: Loss of caveolin-1 gene expression accelerates the development of dysplastic mammary lesions in tumor-prone transgenic mice. *Mol Biol Cell* 2003, 14:1027–1042
- Capozza F, Williams TM, Schubert W, McClain S, Bouzazah B, Sotgia F, Lisanti MP: Absence of caveolin-1 sensitizes mouse skin to carcinogen-induced epidermal hyperplasia and tumor formation. *Am J Pathol* 2003, 162:2029–2039
- Ho CC, Huang PH, Huang HY, Chen YH, Yang PC, Hsu SM: Up-regulated caveolin-1 accentuates the metastasis capability of lung adenocarcinoma by inducing filopodia formation. *Am J Pathol* 2002, 161:1647–1656
- Yang G, Truong LD, Timme TL, Ren C, Wheeler TM, Park SH, Nasu Y, Bangma CH, Kattan MW, Scardino PT, Thompson TC: Elevated expression of caveolin is associated with prostate and breast cancer. *Clin Cancer Res* 1998, 4:1873–1880
- Volonte D, Galbiati F, Lisanti MP: Visualization of caveolin-1, a caveolar marker protein, in living cells using green fluorescent protein (GFP) chimeras: the subcellular distribution of caveolin-1 is modulated by cell-cell contact. *FEBS Lett* 1999, 445:431–439
- Strumane K, Van Roy F, Bex G: The role of E-cadherin in epithelial

- differentiation and cancer progression. *Recent Results Dev Cell Biochem* 2003, 1:33–37
17. Cavallaro U, Christofori G: Cell adhesion and signalling by cadherins and Ig-CAMs in cancer. *Nat Rev Cancer* 2004, 4:118–132
  18. Galbiati F, Volonte D, Brown AM, Weinstein DE, Ben-Ze'ev A, Pestell RG, Lisanti MP: Caveolin-1 expression inhibits Wnt/beta-catenin/Lef-1 signaling by recruiting beta-catenin to caveolae membrane domains. *J Biol Chem* 2000, 275:23368–23377
  19. Lu Z, Ghosh S, Wang Z, Hunter T: Downregulation of caveolin-1 function by EGF leads to the loss of E-cadherin, increased transcriptional activity of beta-catenin, and enhanced tumor cell invasion. *Cancer Cell* 2003, 4:499–515
  20. Daniel JM, Reynolds AB: Tyrosine phosphorylation and cadherin/catenin function. *BioEssays* 1997, 19:883–891
  21. Hu P, O'Keefe EJ, Rubenstein DS: Tyrosine phosphorylation of human keratinocyte beta-catenin and plakoglobin reversibly regulates their binding to E-cadherin and alpha-catenin. *J Invest Dermatol* 2001, 117:1059–1067
  22. Ozawa M, Ohkubo T: Tyrosine phosphorylation of p120(ctn) in v-Src transfected L cells depends on its association with E-cadherin and reduces adhesion activity. *J Cell Sci* 2001, 114:503–512
  23. Sundfeldt K, Piontekewitz Y, Ivarsson K, Nilsson O, Hellberg P, Brännström M, Janson PO, Enerbäck S, Hedin L: E-cadherin expression in human epithelial ovarian cancer and normal ovary. *Int J Cancer* 1997, 74:275–280
  24. Davies BR, Worsley SD, Ponder BA: Expression of E-cadherin, alpha-catenin and beta-catenin in normal ovarian surface epithelium and epithelial ovarian cancers. *Histopathology* 1998, 32:69–80
  25. Marques FR, Fonseca-Carvasan GA, Angelo Andrade LA, Botcher-Luiz F: Immunohistochemical patterns for alpha- and beta-catenin, E- and N-cadherin expression in ovarian epithelial tumors. *Gynecol Oncol* 2004, 94:16–24
  26. Kruk PA, Maines-Bandiera SL, Auersperg N: A simplified method to culture human ovarian surface epithelium. *Lab Invest* 1990, 63:132–136
  27. De Cecco L, Marchionni L, Gariboldi M, Reid JF, Lagonigro MS, Caramuta S, Ferrario C, Bussani E, Mezzanzanica D, Turatti F, Delia D, Daidone MG, Oggioni M, Bertuetti N, Ditto A, Raspagliesi F, Pilotti S, Pierotti MA, Canevari S, Schneider C: Gene expression profiling of advanced ovarian cancer: characterization of molecular signature involving the fibroblast growth factor 2. *Oncogene* 2004, 23:8171–8183
  28. Sargiacomo M, Sudol M, Tang Z, Lisanti MP: Signal transducing molecules and glycosyl-phosphatidylinositol-linked proteins form a caveolin-rich insoluble complex in MDCK cells. *J Cell Biol* 1993, 122:789–807
  29. Miotti S, Bagnoli M, Tomassetti A, Colnaghi MI, Canevari S: Interaction of folate receptor with signaling molecules lyn and  $G_{\alpha 13}$  in detergent-resistant complexes from the ovary carcinoma cell line IGROV1. *J Cell Sci* 2000, 113:349–357
  30. Laemmli UK: Cleavage of structural proteins during the assembly of the head of bacteriophage T4. *Nature* 1970, 227:680–685
  31. Simons K, Toomre D: Lipid rafts and signal transduction. *Nature* 2000, 1:22–30
  32. Adams CL, Nelson WJ, Smith SJ: Quantitative analysis of cadherin-catenin-actin reorganization during development of cell-cell adhesion. *J Cell Biol* 1996, 135:1899–1911
  33. Irby RB, Yeatman TJ: Increased Src activity disrupts cadherin/catenin-mediated homotypic adhesion in human colon cancer and transformed rodent cells. *Cancer Res* 2002, 62:2669–2674
  34. Frame MC: Newest findings on the oldest oncogene: how activated src does it. *J Cell Sci* 2004, 117:989–998
  35. Hanke JH, Gardner JP, Dow RL, Changelian PS, Brissette WH, Weringer EJ, Pollok BA, Connelly PA: Discovery of a novel, potent, and Src family-selective tyrosine kinase inhibitor: study of Lck- and FynT-dependent T cell activation. *J Biol Chem* 1996, 271:695–701
  36. Cerejido M, Robbins ES, Dolan WJ, Rotunno CA, Sabatini DD: Polarized monolayers formed by epithelial cells on a permeable and translucent support. *J Cell Biol* 1978, 77:853–880
  37. Le TL, Yap AS, Stow JL: Recycling of E-cadherin: a potential mechanism for regulating cadherin dynamics. *J Cell Biol* 1999, 146:219–232
  38. Aghib DF, McCrea PD: The E-cadherin complex contains the src substrate p120. *Exp Cell Res* 1995, 218:359–369
  39. Lee H, Park DS, Razani B, Russell RG, Pestell RG, Lisanti MP: Caveolin-1 mutations (P132L and null) and the pathogenesis of breast cancer: caveolin-1 (P132L) behaves in a dominant-negative manner and caveolin-1 (–/–) null mice show mammary epithelial cell hyperplasia. *Am J Pathol* 2002, 161:1357–1369
  40. Sloan EK, Stanley KL, Anderson RL: Caveolin-1 inhibits breast cancer growth and metastasis. *Oncogene* 2004, 23:7893–7897
  41. Williams TM, Medina F, Badano I, Hazan RB, Hutchinson J, Muller WJ, Chopra NG, Scherer PE, Pestell RG, Lisanti MP: Caveolin-1 gene disruption promotes mammary tumorigenesis and dramatically enhances lung metastasis in vivo: Role of Cav-1 in cell invasiveness and matrix metalloproteinase (MMP-2/9) secretion. *J Biol Chem* 2004, 279:51630–51646
  42. Bagnoli M, Canevari S, Figini M, Mezzanzanica D, Raspagliesi F, Tomassetti A, Miotti S: A step further in understanding the biology of the folate receptor in ovarian carcinoma. *Gynecol Oncol* 2003, 88:140–144
  43. Auersperg N, Wong AS, Choi KC, Kang SK, Leung PC: Ovarian surface epithelium: biology, endocrinology, and pathology. *Endocr Rev* 2001, 22:255–288
  44. Singer G, Kurman RJ, Chang HW, Cho SK, Shih I: Diverse tumorigenic pathways in ovarian serous carcinoma. *Am J Pathol* 2002, 160:1223–1228
  45. Furlong MT, Morin PJ: Rare activation of the TCF/beta-catenin pathway in ovarian cancer. *Gynecol Oncol* 2000, 77:97–104
  46. Nusrat A, Parkos CA, Verkade P, Foley CS, Liang TW, Innis-Whitehouse W, Eastburn KK, Madara JL: Tight junctions are membrane microdomains. *J Cell Sci* 2000, 113:1771–1781
  47. Fujita Y, Krause G, Scheffner M, Zechner D, Leddy HE, Behrens J, Sommer T, Birchmeier W: Hakai, a c-Cbl-like protein, ubiquitinates and induces endocytosis of the E-cadherin complex. *Nat Cell Biol* 2002, 4:222–231
  48. Palacios F, Price L, Schweitzer J, Collard JG, D'Souza-Schorey C: An essential role for ARF6-regulated membrane traffic in adherens junction turnover and epithelial cell migration. *EMBO J* 2001, 20:4973–4986
  49. Avizienyte E, Wyke AW, Jones RJ, McLean GW, Westhoff MA, Brunton VG, Frame MC: Src-induced de-regulation of E-cadherin in colon cancer cells requires integrin signalling. *Nat Cell Biol* 2002, 4:632–638
  50. Seidel B, Braeg S, Adler G, Wedlich D, Menke A: E- and N-cadherin differ with respect to their associated p120ctn isoforms and their ability to suppress invasive growth in pancreatic cancer cells. *Oncogene* 2004, 23:5532–5542
  51. Thoreson MA, Reynolds AB: Altered expression of the catenin p120 in human cancer: implications for tumor progression. *Differentiation* 2002, 70:583–589
  52. Daniel JM, Spring CM, Crawford HC, Reynolds AB, Baig A: The p120(ctn)-binding partner Kaiso is a bi-modal DNA-binding protein that recognizes both a sequence-specific consensus and methylated CpG dinucleotides. *Nucleic Acids Res* 2002, 30:2911–2919
  53. Sario D, Perez-Mies B, Hardisson D, Moreno-Bueno G, Suarez A, Cano A, Martin-Perez J, Gamallo C, Palacios J: Cytoplasmic localization of p120ctn and E-cadherin loss characterize lobular breast carcinoma from preinvasive to metastatic lesions. *Oncogene* 2004, 23:3272–3283
  54. Owens DW, McLean GW, Wyke AW, Paraskeva C, Parkinson EK, Frame MC, Brunton VG: The catalytic activity of the Src family kinases is required to disrupt cadherin-dependent cell-cell contacts. *Mol Biol Cell* 2000, 11:51–64
  55. Summy JM, Gallick GE: Src family kinases in tumor progression and metastasis. *Cancer Metastasis Rev* 2003, 22:337–358
  56. Pengetnze Y, Steed M, Roby KF, Terranova PF, Taylor CC: Src tyrosine kinase promotes survival and resistance to chemotherapeutics in a mouse ovarian cancer cell line. *Biochem Biophys Res Commun* 2003, 309:377–383
  57. Wiener JR, Windham TC, Estrella VC, Parikh NU, Thall PF, Deavers MT, Bast RC, Mills GB, Gallick GE: Activated SRC protein tyrosine kinase is overexpressed in late-stage human ovarian cancers. *Gynecol Oncol* 2003, 88:73–79
  58. Li S, Couet J, Lisanti MP: Src tyrosine kinases, Galpha subunits, and H-Ras share a common membrane-anchored scaffolding protein, caveolin: caveolin binding negatively regulates the auto-activation of Src tyrosine kinases. *J Biol Chem* 1996, 271:29182–29190